

Article

Estimating Urbanization's Impact on Soil Erosion: A Global Comparative Analysis and Case Study of Phoenix, USA

Ara Jeong ^{1,*}, Dylan S. Connor ², Ronald I. Dorn ² and Yeong Bae Seong ³

¹ Department of Geography, College of Sciences, Kyung Hee University, Seoul 02447, Republic of Korea
² School of Geographical Sciences and Urban Planning, Arizona State University, Tempe, AZ 85287, USA; d.c@asu.edu (D.S.C.); atrid@asu.edu (R.I.D.)
³ Department of Geography, Korea University, Seoul 02841, Republic of Korea; ybseong@korea.ac.kr
* Correspondence: ara.jeong@khu.ac.kr

Abstract

Healthy soils are an essential ingredient of land systems and ongoing global change. Urbanization as a global change process often works through the lens of urban planning, which involves urban agriculture, urban greening, and leveraging nature-based solutions to promote resilient cities. Yet, urbanization frequently leads to soil erosion. Despite recognition of this tension, the rate at which the urban growth boundary accelerates soil erosion above natural background levels has not yet been determined. Our goal here is to provide a first broad estimate of urbanization's impact of soil erosion. By combining data on modern erosion levels with techniques for estimating long-term natural erosion rates through cosmogenic nuclide ¹⁰Be analysis, we modeled the impact of urbanization on erosion across a range of cities in different global climates, revealing an acceleration of soil erosion ~7–19x in environments with mean annual precipitation <1500 mm; growth in wetter urban centers accelerated soil erosion ~23–72x. We tested our statistical model by comparing natural erosion rates to decades of monitoring soil erosion on the margins of Phoenix, USA. A century-long expansion of Phoenix accelerated soil erosion by ~12x, an estimate that is roughly at the mid-point of model projections for drier global cities. In addition to urban planning implications of being able to establish a baseline target of natural rates of soil erosion, our findings support the urban cycle of soil erosion theory for the two USA National Science Foundation urban long-term ecological research areas of Baltimore and Phoenix.

Keywords: urban soil; background rates of soil erosion; sustainable landscape pattern; urban agriculture; urban greening; urban nature-based solutions



Academic Editors: Le Yu, Xin Chen, Zhenrong Du and Pengyu Hao

Received: 10 July 2025

Revised: 1 August 2025

Accepted: 1 August 2025

Published: 4 August 2025

Citation: Jeong, A.; Connor, D.S.; Dorn, R.I.; Seong, Y.B. Estimating Urbanization's Impact on Soil Erosion: A Global Comparative Analysis and Case Study of Phoenix, USA. *Land* **2025**, *14*, 1590. <https://doi.org/10.3390/land14081590>

Copyright: © 2025 by the authors. Licensee MDPI, Basel, Switzerland. This article is an open access article distributed under the terms and conditions of the Creative Commons Attribution (CC BY) license (<https://creativecommons.org/licenses/by/4.0/>).

1. Introduction

This Special Issue focuses on observation and modeling of land system changes, with the goal of presenting new data and models. We do both in this paper, focusing on the land system change in urban growth's impact on soil erosion. However, the reader should be cognizant that this is the first research designed to quantify just how much urbanization accelerates soil erosion above natural background rates. As such, our goal is not to provide a hard and firm rate of acceleration, but a first approximation.

Urban soils are part of global human-driven land use change [1–3]. Soils provide ecosystem services both within and outside cities, such as carbon storage and its association with global climate regulation [4,5], effective stormwater management [6,7], and

regulation of the urban heat island effect [8,9]. Urban soils play an important role in urban planning [10]. However, urban soils are sometimes an overlooked resource in human adaptation to global and local environmental changes [11].

Urbanization, while providing essential infrastructure and services for growing populations, has a profound impact. Urban growth alters temperature [12], vegetation [13], carbon emissions [14], and many other effects. The focus on this paper rests on the role of urban expansion on urban soils.

In this context, the process of urbanization directly impacts the erosion dynamics of urban soils. The modification of natural landscapes through construction and development accelerates soil erosion, shifting the location and magnitude of erosion patterns. A half-century ago, Wolman [15] proposed the “urban cycle of erosion” model for understanding how urbanization influences soil erosion, specifically for the Baltimore/Washington D.C. area, USA. His iconic schematic diagram illustrates how sediment yield changes over time as urban development transforms a humid, vegetated landscape, altering hydrologic flow paths and accelerating soil erosion (Figure 1). This model emphasizes the need to understand and address the impacts of urbanization on soil erosion to mitigate its consequences and protect vital ecosystem services provided by urban soils. It has not been possible to quantify the acceleration of soil erosion from urbanization until now.

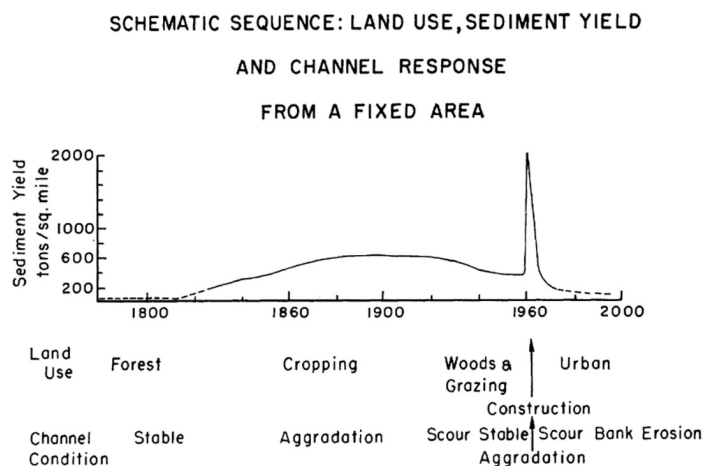


Figure 1. Wolman’s [15] hypothesized cycle of erosion associated with urbanization. (Reproduced from [15]).

Thus, a significant research gap persists in determining specific criteria or thresholds for reducing soil erosion in urban areas. The reason why we focus on urban planning in this paper is that soil erosion might best be managed in an urban context by planners. Unfortunately, no data exists for the appropriate erosion reduction targets that should be established, nor on whether these targets should be tailored to the unique characteristics of different urban environments. Furthermore, it remains unclear whether the same erosion reduction values should be applied universally across cities or whether strategies should be adapted to the specific climatic conditions of each urban setting. Consequently, there is a lack of research that bridges the gap between scientific understanding of accelerated soil erosion due to urbanization and its practical implementation. This gap particularly pertains to providing evidence-based recommendations.

These unresolved issues give rise to several critical research questions: (i) How can the pre-Anthropocene (pre-human impact) erosion rate be quantified to provide target erosion rates for urban planners? (ii) How can urban planners effectively assess the current status of soil erosion acceleration in urban environments? (iii) How should erosion reduction targets be adapted to account for the unique characteristics of different urban environments?

Our approach to address this gap uses ^{10}Be (Beryllium-10) catchment-averaged erosion rates. The long half-life of ^{10}Be (1.387 million years) enables the calculation of long-term average erosion rates over periods ranging from 1000 to 100,000 years. These long-term erosion rates provide a natural baseline for understanding erosion dynamics in undisturbed landscapes. By establishing such a baseline, urban planners can use these values as reference points for setting target erosion rates [16,17], thereby informing the development of more effective strategies to manage and mitigate soil erosion in urban settings. In addition, comparing ^{10}Be -derived erosion rates, which represent the natural baseline, to current soil erosion rates can provide valuable insights into the extent of urbanization's impact on soil erosion. Expressed as a ratio (i.e., urban erosion rates relative to natural background levels), this comparison offers urban planners a practical framework for effectively managing and controlling soil erosion in urban areas.

To address the research questions outlined above and to meet the goal of this Special Issue by presenting both new observations and modeling, we designed our study in several steps (Figure 2). First, we analyze prior published compilations of ^{10}Be natural background erosion rates using the catchment-averaged denudation rate (CADR) method [18], alongside the compilation by Russell et al. [17] on modern urban soil erosion. This analysis involves developing a statistical model for global cities to estimate the acceleration of erosion in urban environments across different contexts. One limitation of our approach is that CADR data are not derived from the same global urban catchments as those compiled by Russell et al. [17]. To mitigate this, we use nearby catchments or estimates from similar climates. However, we acknowledge that more accurate estimates will be possible in the future through data sampled from the same urban sites.

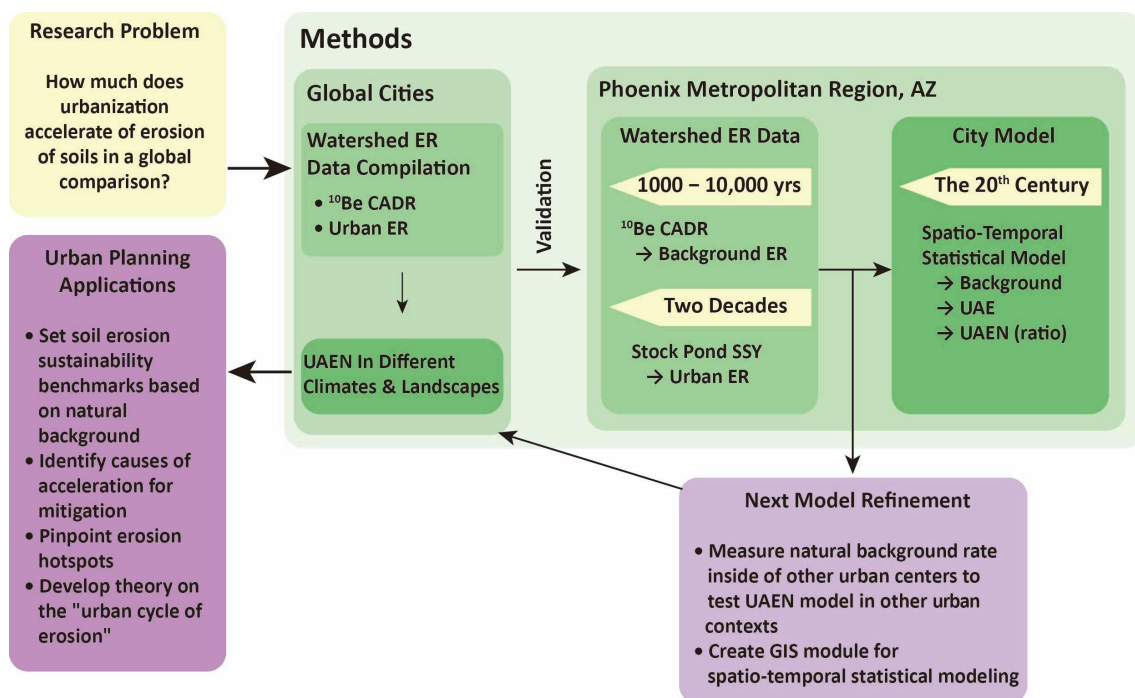


Figure 2. Overview of the research question, methods, scales, intended results, urban planning applications, and next steps for model refinement. ER: Erosion Rate; CADR: Catchment-Averaged Denudation Rate; SSY: Area-Specific Sediment Yield; UAE: Urban-Accelerated Erosion Rate; UAEN: Urban Acceleration of Erosion above Natural Background (ratio).

Our new data come from Phoenix, Arizona, USA. Located in the Sonoran Desert, Phoenix has been an icon of sprawl in urban planning [19], and more recently discussed in planning for urban heat resilience [20]. This urban sprawl, however, has been an important

aspect of our ability to measure CADR and monitor urban soil erosion using the same watersheds. Jeong et al. [21] provided CADR data for watersheds that have experienced over two decades of urban sprawl in Phoenix Metropolitan Region (PMR), and these watersheds were previously studied for urban soil erosion [22]. We utilize these watershed-specific results to develop a statistical model of natural background erosion rates for the entire PMR, based on the CADR data. Subsequently, we present the first approximation of a spatiotemporal statistical model for the rate of urban-accelerated erosion (UAE) in PMR, using two decades of soil erosion data. Finally, we combine the CADR and UAE models to present the first model of urbanization’s acceleration of soil erosion above natural background (UAEN). Our Phoenix-wide statistical model serves as a test of the validity of the global cities model across both space and time.

Phoenix, thus, presents a particularly valuable case study for two reasons. First, the 2023 U.S. Census confirmed that Phoenix is now the fifth largest city in the United States [23], and it is the fastest growing of the major U.S. cities. Second, Phoenix is one of two urban centers selected by the U.S. National Science Foundation for long-term ecological research, representing an arid region, alongside the Baltimore/Washington D.C. area, which serves as a representative temperate humid region [24,25]. Therefore, our global comparative analysis and the specific results for Phoenix will contribute to urban soil sustainability by: (a) presenting a model to measure urban acceleration of erosion above natural background rates; and (b) offering a framework for understanding soil erosion across an important urban region using watershed-specific data.

In the Discussion section (Section 5), we return to how our approach to quantifying the impact of urban growth on erosion can be applied to promote sustainable urban landscape patterns. Our research strategy links spatial patterns of land use and land cover change in urbanizing cities to the processes and rates of soil erosion. By considering regional social-ecological elements, we attempt to work towards “sustainable development goals” (cf. [26], p. 1843), contributing to spatial environmental planning efforts aimed at fostering healthy urban soils.

2. Study Areas

We selected our sample of global cities (Figure 3) to understand soil erosion based on two very different published datasets: (i) urban areas where Russell et al. [17] compiled available data on urbanization’s impact on soil erosion; and (ii) nearby watersheds where ^{10}Be CADR data are available [27,28], or watersheds with CADR data with similar slopes and climate to matching urban area [29]. Figure 3 also includes our case study urban area of Phoenix, Arizona, USA.

Table 1. Mean slope of different global cities. Supplementary File S1 presents the slope maps used to analyze the mean slope of these cities. The urban ID number corresponds with Figure 3, Table S1 in Supplementary File S2, and Supplementary File S1. Cities 1 through 8 (bold and *) in Table 1 are those we analyzed because they have both nearby/related ^{10}Be CADR data and low slopes. The other cities listed are ripe targets for future studies using ^{10}Be .

ID	City Name	Mean slope (°)	Std (°)
1	West Fork, Arkansas, USA *	4.5	3.6
2	Washington D.C., USA *	3.7	3.0
3	Phoenix, Arizona, USA *	4.0	3.2
4	Fredericksburg, Virginia, USA *	3.4	3.2
5	Haean-myeon, South Korea *	7.1	4.5
6	Kuala Lumpur, Malaysia *	4.5	5.0
7	Tokyo, Japan *	2.4	2.7

Table 1. Cont.

ID	City Name	Mean slope (°)	Std (°)
8	Guwahati, India *	2.7	4.4
9	Bogota, Columbia	2.8	3.7
10	Rome, Italy	3.8	3.4
11	El Alto-La Paz, Bolivia	5.1	6.8
12	Nairobi, Kenya	3.2	2.6
13	Addis Ababa, Ethiopia	4.7	3.6
14	Mexico City, Mexico	3.5	4.4
15	Quito, Ecuador	8.2	7.1
16	Santiago, Chile	1.8	1.9
17	Sana'a, Yemen	2.0	2.0
18	Tehran, Iran	3.3	3.1
19	Kabul, Afghanistan	2.7	4.9
20	Ankara, Turkey	5.9	4.9
21	Chongqing, China	7.8	6.7
22	Stockholm, Sweden	4.1	4.2
23	Zurich, Switzerland	4.8	4.4
24	Berlin, Germany	1.3	1.3
25	London, UK	2.2	2.3
26	Paris, France	2.5	2.6
27	Sydney, Australia	4.0	3.8
28	Toronto, Canada	2.3	2.4
29	Beijing, China	2.3	3.2
30	Seoul, South Korea	6.0	6.3

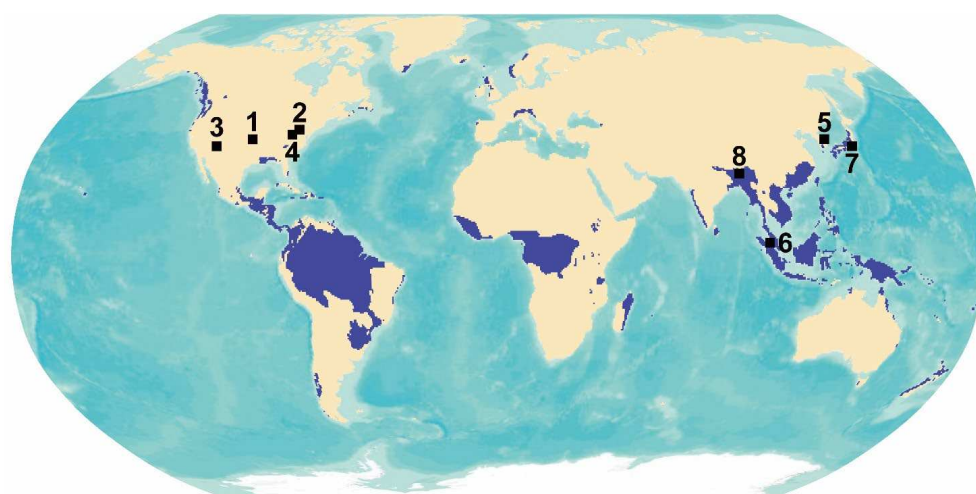


Figure 3. Locations of urban areas analyzed in this paper. Numbers correspond with the city ID in Table 1. The regions with mean annual precipitation >1500 mm [30] are blue-colored. The base map was imported from ESRI, producer of ArcGIS software 10.7.1 and public datasets—accessed through the Arizona State University license. Note—1: West Fork, Arkansas, USA; 2: Washington D.C., USA; 3: Phoenix, Arizona, USA; 4: Fredericksburg, Virginia, USA; 5: Haean-myeon, South Korea; 6: Kuala Lumpur, Malaysia; 7: Tokyo, Japan; 8: Guwahati, India.

The selection of appropriate cities had to be constrained by an urban slope. Cities with very steep slopes experience landslides and other mass wasting processes, as well as gullying. Since these processes can invalidate the ^{10}Be CADR method of determining natural rates of erosion, our selection of cities must exclude cities with mean slopes above 8.5° [31]. The ^{10}Be CADR method is based on erosion that happens first when rainfall generates rainsplash erosion [32]. Then, water that does not infiltrate continues to erode exposed ground via overland flow that picks up loose particles [33,34]. Thus, to compare

global cities with similar basic geomorphic conditions, we identified major global cities with mean slopes below 8.5° (see Supplementary File S1 for slope maps), which we present in Table 1.

The values presented in Table 1 go beyond this particular study, because they offer potential future urban regions that would be most amenable for further study using our methodological approach. Thus, Table 1 includes more cities than we analyze here, because (i) we needed to understand first what cities had average slopes below the key threshold of 8.5° that would indicate the dominant erosion processes on bare ground would be rain splash and overland flow; (ii) match these cities with existing data on modern urban erosion (e.g., [17]); and then (iii) match those cities that had nearby CADR data on background erosion rates [27,28], or had comparable natural watersheds in terms of slope and climate with CADR data [29]. Cities 1 through 8 in Table 1 and Figure 3 met these three conditions. Hence, the cities in Figure 3 are used in the development of a statistical model to compare existing urban erosion data with existing CADR background soil erosion rates.

For the PMR (Figure 4), we collected our own data on both modern rates of soil erosion due to urbanization [22] and ^{10}Be CADR [21]. This was necessary because we needed to measure modern urban soil erosion from the same watersheds as those used for CADR in order to assess the accuracy of the modeling conducted for other global cities (Figure 3).

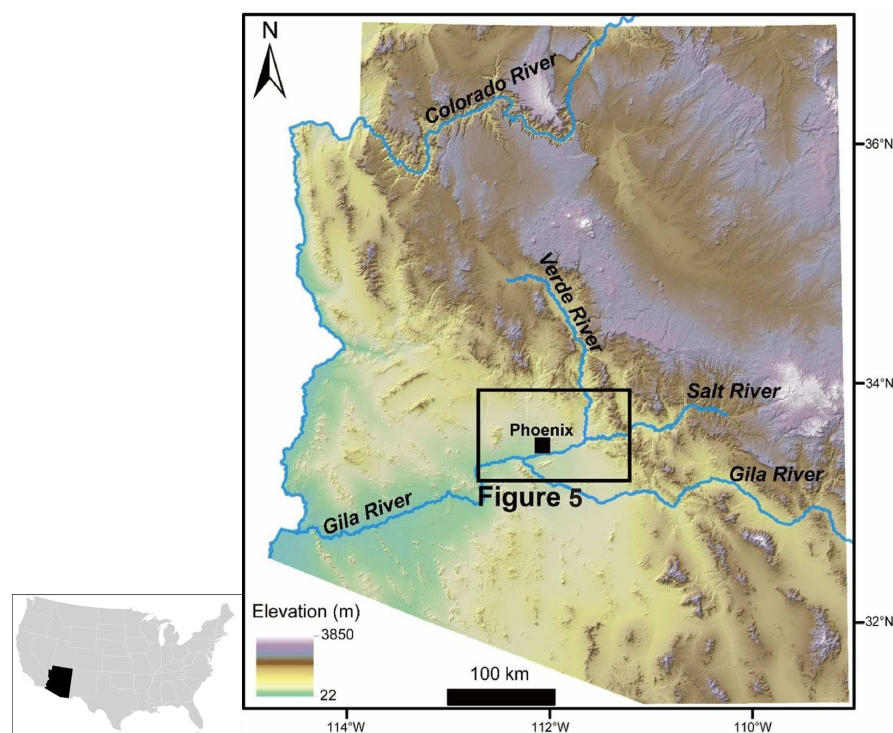


Figure 4. The metropolitan Phoenix region, identified by the rectangular box and the location of downtown Phoenix indicated by the solid square—placed with the context of the State of Arizona, USA. Phoenix could develop in such an arid, hot region because of its large drainage area that supplies gravity-fed water from mountains to the north and east.

Figure 5 contextualizes the locations of these watersheds monitored CADR and also erosion rates for over two decades, as the expanding PMR progressively encroached upon the surrounding Sonoran Desert. Soil erosion was monitored as it progressed through different stages, beginning with cattle grazing, followed by impacts from wildfire, and ultimately leading to the exposure of bare ground due to urbanization [22]. Subsequently, ^{10}Be CADR measurements were taken from the same watersheds [21], enabling the first direct comparison of urbanization-induced erosion to natural background erosion.

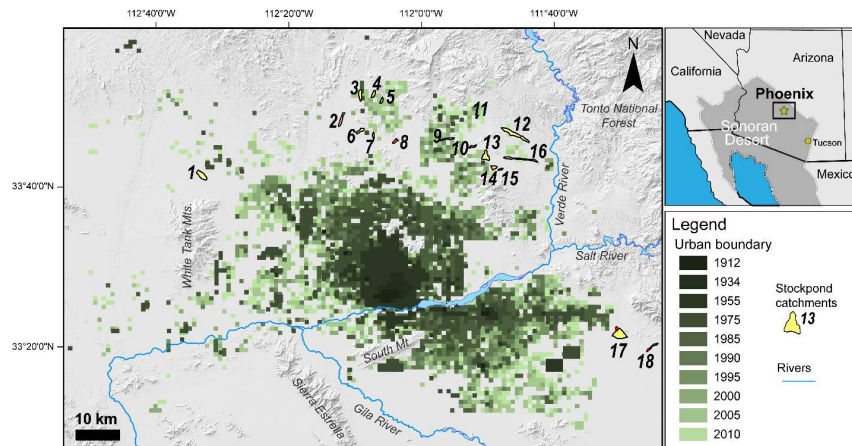


Figure 5. Urban sprawl of Phoenix metropolitan region contextualizing the scattered locations of 18 monitored stock pond catchments with urban sprawl from 1912 to 2010. Urban boundaries were extracted from land cover classification by Central Arizona–Phoenix Long-Term Ecological Research. Numbers refer to catchments identified prior research [21,22] and in Supplementary File S3 that presents all of these watersheds (by number and by name), their land use histories, precipitation, and erosion data.

Figure 6 illustrates how soil erosion was influenced by land use and land cover changes (LULCC) in one of these watersheds. For each watershed, we analyzed historical aerial photographic imagery to identify timelines of LULCC (exemplified by Figure 6A for one of the Phoenix-region watersheds). We then developed a method to quantify aerial changes in LULCC across different time periods for each watershed (Figure 6B). After completing the erosion data analysis, we compared LULCC to natural background erosion rates (CADR), as exemplified by Figure 6C. Supplementary File S3 provides this same analysis for all 18 monitored watersheds.

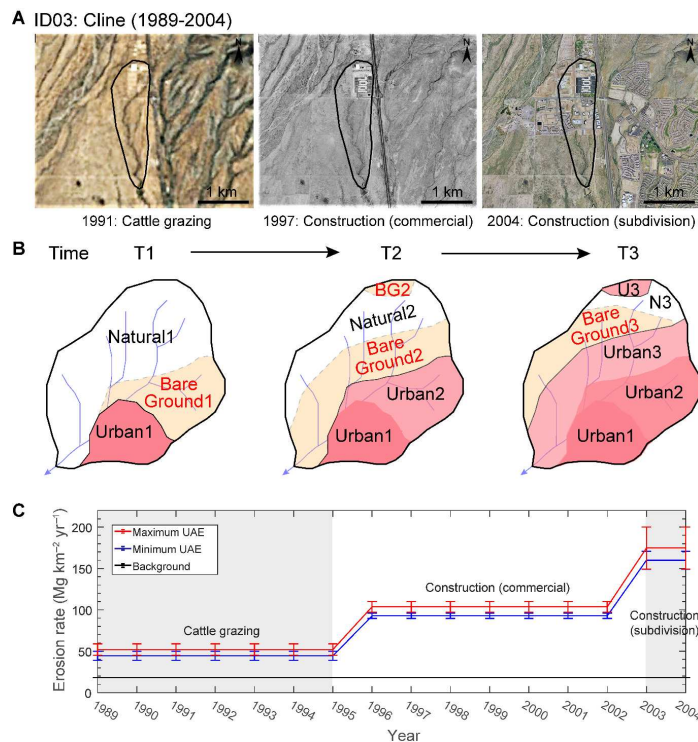


Figure 6. An example of how urbanization impacted a Phoenix-region watershed monitored for both natural background soil erosion (dark black line) and the influence of land use changes. The ID of this watershed is ID3 in prior research [21,22]. (A) LULCC of Cline stock pond catchment illustrated in

aerial photographs. (B) Idealized explanation of how we calculated bare ground exposure (modified from Jeong [35]). The dashed line is the imaginary line that does not exist on the land use/land cover classification map, which is to show the exposed bare ground. The exposed bare ground during the time period from T1 to T2 (Bare Ground1) can be calculated by the intersection of natural land cover in T1 (Natural1) and urban land cover in T2 (Urban2). The annual urban growth was calculated from dividing by the length of time period. (C) Comparison between CADR natural background soil erosion (lower flat line) with pre-urbanization cattle grazing and then urban development between 1989 to 2004.

3. Methods

Our approach to estimating the impact of urbanization on soil erosion above natural background (UAEN) differs topically from the air quality research of Yao et al. [36], but it shares methodological similarities, particularly in the use of a space-time regression model that explores physical geography data across an urban region. This section outlines six key steps, two of which we have been discussed in prior work: (i) measuring ^{10}Be CADR on timescales of 10^3 – 10^5 years from the PMR watersheds to obtain natural background rates of erosion [21]; and (ii) collecting and analyzing two decades of soil erosion data from the same PMR watersheds used for CADR [22]. Our data collection process spanned over two decades and incorporated significant LULCC, including transitions from cattle grazing to urbanization-induced bare ground exposure, as well as the impacts of wildfires.

This paper documents the four remaining tasks required to compare the CADR, which provides a sustainability target [21], with the impact of urbanization on soil sustainability. These four tasks are summarized in this section, with extensive details on data collection and methods provided in Supplementary File S2. The information in Supplementary File S2 offers a new set of tools for researchers aiming to further investigate urban soil sustainability.

The sequence of methods summarized here begins by modeling CADR for various global cities where urban soil erosion data have already been compiled. Next, we model natural background erosion rates for the entire PMR using the CADR data. Third, we present a model for the rate of UAE in the PMR, based on two decades of soil erosion data. Fourth, we compare UAE to CADR to develop a model of UAEN for the PMR. This Phoenix-specific case study enables us to test the accuracy of the global cities model.

Before delving into the details, we wish to stress that our findings are ultimately limited by the lack of data on background rates of soil erosion in global cities outside of Phoenix, Arizona, USA. The limitations of our methods expressed in the sections that follow also mean that our results are best interpreted as broad estimates of how urban growth increases soil erosion.

3.1. Comparison of UAEN to Global Cities in Different Environmental Settings

We compiled global scholarship from CADR research [27–29] to compare with modern sediment yields from urban centers undergoing substantial urban expansion [17]. This approach enabled the first comparison of sediment yields impacted by urban-accelerated erosion (UAE) and natural background erosion.

A significant challenge, however, is the lack of CADR data for the same watersheds studied for urban soil erosion. While CADR data may exist for nearby catchments or similar climatic regions, only one urban location—within the Potomac River basin of Chesapeake Bay, USA—had both CADR and modern urban soil erosion rates [28,37]. Importantly, neither of these studies was designed to compare natural and urban soil erosion.

Given this limitation, we focused on locations with reported median sediment yields from urbanizing catchments (as referenced in [17], and detailed Table S1 in Supplementary File S2). The scarcity of CADR data from the same catchments prevented direct comparison. Therefore, we utilized nearby CADR data or, in cases where such data were unavailable,

employed the median CADR values from multiple studies conducted in similar climate regimes [29]. Section S2 in Supplementary File S2 provides further details on how we addressed key discrepancies across studies.

To compare our findings in the PMR, we limited our analysis to cities with basic geomorphic conditions similar to Phoenix, specifically: (i) mean slopes below 8.5° [31] (Supplementary File S1 presents slope maps for 30 such global cities); and (ii) where eroded soil primarily results from overland flow processes, rather than gullying or streambed erosion. The 8.5° threshold is a reasonable one for the PMR, since gullying tends to occur on steeper slopes. While previous studies [16,17] emphasize that processes other than rainsplash and overland flow contribute to erosion in various urban contexts, we focused on low-slope cities to enhance the likelihood of comparing similar geomorphic erosion processes. We acknowledge that our global erosion assessment is subject to high uncertainty, due to the insufficient availability of CADR data for urbanizing catchments.

3.2. Natural Background of Soil Erosion Rates

Controlled experiments have previously determined that CADR is insensitive to urbanization-induced soil erosion in the PMR [21]. Jeong et al. [21] collected active-channel sediment samples from 18 stock pond watersheds that had undergone urbanization over the past two decades. The CADR of each stock pond watershed is presented in Jeong et al. [21]. To compare CADR with modern sediment yields, bedrock density was used for conversion from length unit to mass unit (e.g., $\text{m My}^{-1} \times \text{bedrock density}$, $2.7 \text{ t m}^{-3} = \text{Mg km}^{-2} \text{ yr}^{-1}$).

Jeong et al. [21] collected active-channel sediment samples from 18 stock pond watersheds that had undergone urbanization over the past two decades. The CADR for each watershed are presented in Jeong et al. [21]. To compare CADR with modern sediment yields, bedrock density was used to convert from length units to mass units (e.g., $\text{m My}^{-1} \times \text{bedrock density of } 2.7 \text{ t m}^{-3} = \text{Mg km}^{-2} \text{ yr}^{-1}$).

3.3. Modern Rates of Soil Erosion

To understand erosion associated with different LULCC over time in the PMR (Figure 5), sediment accumulation depths were measured from 18 stock ponds during the expansion of Phoenix's urban fringe between 1989 and 2013 [22] (Figures 4 and 5). Since dust storms are common in the Phoenix region, the silt and clay accumulating in the stock ponds could potentially originate from aeolian dust deposition, weathered bedrock or, more likely, a combination of these sources. Consequently, two area-specific sediment yields (SSY) (and erosion rates) are presented in Table S5 in Supplementary File S2. The maximum SSY calculation assumes no aeolian dust deposition, while the minimum SSY calculation assumes that all silt and clay are derived from aeolian deposition. SSY was calculated as follows [38]:

$$SSY = SM_{max \text{ or } min} / (A_D \times TE \times Y) \times 10^6 \quad (1)$$

where SSY ($\text{Mg km}^{-2} \text{ yr}^{-1}$) is the area-specific sediment yield, SM (Mg) is sediment mass, A_D (km^2) is drainage area of the watershed of each stock pond, TE (%) is the sediment trap efficiency (100% for each stock pond) and Y (years) is the measurement period. The maximum sediment mass (SM_{max}) and minimum sediment mass (SM_{min}) were calculated as follows:

$$SM_{max} = SV \times dBD = A_p \times D_{avg} \times dBD, \quad (2)$$

$$SM_{min} = SM_{max} \times (1 - \text{percent silt and clay}) \quad (3)$$

where SV (m^3) is the measured sediment volume in the stock pond during the given time period Y (years), dBD (t m^{-3}) is average dry bulk density of the sediment, A_p (m^2) is

sedimentation area and D_{avg} (m) is the averaged depth of the sediments measured from nine grid points. The error term of two sediment yields derives from the standard deviation of nine depth measurements for each time slice. This standard deviation of the average depth then translates as a \pm percentage of the reported sediment yield.

We followed previous studies in comparing CADR and modern SSY [39,40], using the bedrock density ($\sim 2.7 \text{ g cm}^{-3}$) for CADR conversion and sediment bulk density for modern SSY calculation (see Table 1 in [21]).

3.4. Modeling Background Rates of Erosion for the Entire Phoenix Metropolitan Region

Jeong et al. [21] demonstrated that natural background rates of erosion were significantly and positively correlated with mean slope ($r = 0.75$, $p < 0.05$) and mean elevation ($r = 0.63$, $p < 0.05$) in the 18 monitored watersheds in PMR. Given that mean slope and mean elevation are significantly correlated and endogenously related [21], we omitted mean elevation as a predictor for natural background sediment yield to mitigate multicollinearity issues. Therefore, mean slope was finally adopted as a proxy for background erosion, as explained in Section S3 of Supplementary File S2.

The final model to predict background erosion for bare ground exposed during the PMR urban expansion from 1912 to 2010 within a regression framework as follows ($R^2 = 0.57$):

$$\text{Background erosion} = 47.677 \times (\text{mean slope}) - 0.075 \quad (4)$$

Full details are provided in Table S2 in Supplementary File S2.

3.5. Modeling Urban Acceleration of Erosion for the Entire Phoenix Metropolitan Region

There are different approaches to modeling soil erosion over a region. The Revised Universal Soil Loss Equation (RUSLE) within a GIS environment usually yields accurate results for watersheds [41–44] and urban landscapes [45–47]. However, given the nature of our historic and cosmogenic nuclide datasets, which exhibit spatiotemporal heterogeneities, we determined that a nested spatiotemporal statistical regression model—similar to those used to study urban air pollution [36,48]—would be more suitable for investigating soil erosion at the urban growth boundary [49].

To model urban acceleration of erosion for bare ground exposed during PMR urban expansion from 1912 to 2010, we examined relationships between modern SSY from the 18 stock ponds, LULCC, and catchment geomorphological factors (i.e., initial urban cover, annual urban growth rate, drainage area, mean slope, relief, and drainage density) (Figure S3 and Table S6 in Supplementary File S2). Through the correlational analysis, we selected annual urban growth rate (AUGR2, in $\text{km}^2 \text{ yr}^{-1}$) and mean slope as proxies for urban acceleration of erosion (Table S7 in Supplementary File) (rationale explained in Section S4 of Supplementary File S2). The final model predicts the urban acceleration of erosion (UAE) within a multiple regression framework as follows (adjusted $R^2 = 0.17$):

$$\text{Urban acceleration of erosion} = 783.92 \times (\text{AUGR2}) + 8.8 \times (\text{mean slope}) + 96.52 \quad (5)$$

Full details are provided in Table S7 in Supplementary File S2.

3.6. Urban Cycle of Erosion for an Arid Environment

Wolman [15] proposed the first and only conceptual model illustrating how LULCC associated with urbanization impact soil erosion. He introduced the concept of the “urban erosion cycle” for the Maryland piedmont, USA, where deforestation and agriculture at the urban growth boundary accelerated erosion. However, this acceleration was not as significant as the erosion observed during the construction phase of urbanization. After

the completion of urbanization, erosion rates decreased substantially with the paving of surfaces [50]. Two critical components of Wolman’s model were based on assumptions due to data limitations: Wolman lacked the ability to measure natural background erosion rates, and he did not account for the urban acceleration of erosion due to surface sealing, such as the application of asphalt and concrete.

While Wolman’s model focused on a humid-region city, we are in a unique position to examine whether a similar “cycle” exists in an arid-region city. To investigate this, we compiled all previously published SSY data in the Köppen–Geiger BWh climate (hot desert climate) setting, as well as data from the PMR [21,22,51]. We categorized the SSY data according to LULC types, including natural, grazing, agriculture, wildfires, construction, and surface sealing. Using these data, we created box-and-whisker plots for each LULC type in arid settings and compared the results with Wolman [15]’s erosion cycle in humid regions.

Table S1 in Supplementary File S4 provides the data on the stock pond catchments necessary for calculating soil erosion, along with other watershed characteristics used in modeling soil erosion in the PMR. Additionally, Table S1 presents the LULC categories. Table S2 in Supplementary File S4 presents summary statistics of compiled SSY data used for the box-and-whisker plot, along with their corresponding references.

4. Results

4.1. Modeling of UAEN for Global Cities in Different Environmental Settings

The global cities UAEN model indicated a similar range of soil erosion acceleration in urban areas, spanning from 200 mm to approximately 1300 mm of mean annual precipitation (MAP). Figure 7 illustrates this range, showing UAEN values between 7x and 19x for cities with MAP <1500 mm. The acceleration of erosion in urban areas increases significantly in cities with MAP >1500 mm, where the modeled UAEN values range from 23x to 72x (Figure 7). These results suggest a three- to four-fold increase in urban-accelerated erosion in wetter climates compared to drier ones.

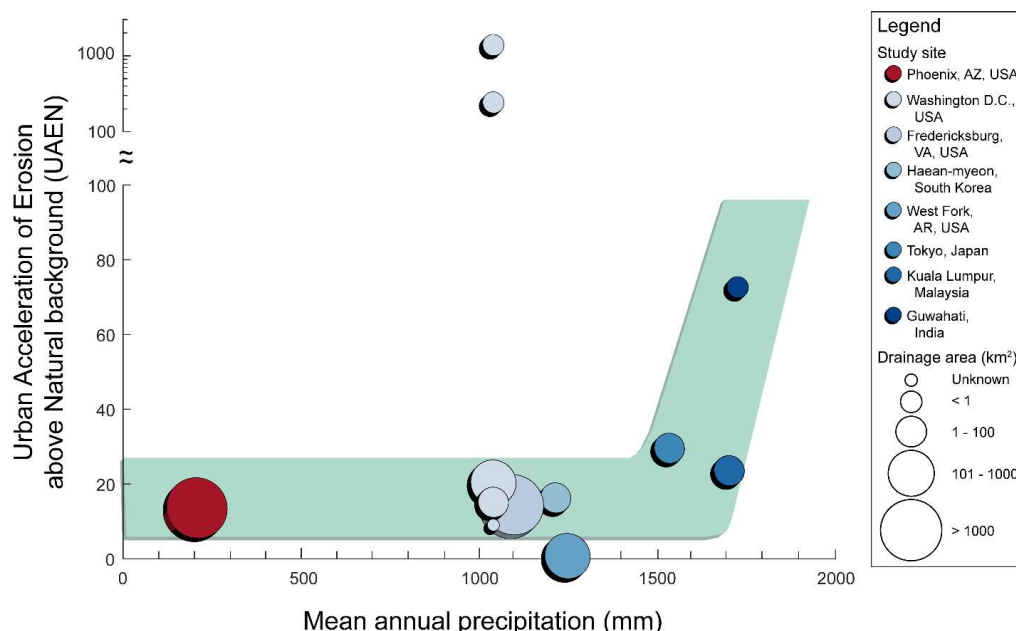


Figure 7. Modeled urban acceleration of erosion above natural background (UAEN) of global cities plotted against mean annual precipitation (MAP). The green shaded area is a visual guide and does not represent a statistically fitted line or confidence interval. The vertical scale is linear up to 100 UAEN and log afterwards. Colors reflect MAP, and size indicates the size of the drainage area.

We offer speculative explanations for the three outliers in Figure 7. The two Washington D.C. subcatchments, which exhibit significantly higher UAEN, may be influenced by gullying, a process known to greatly accelerate erosion. The notably lower UAEN for West Fork, Arkansas, USA, could be attributed to rapid vegetation regrowth at construction sites. These hypotheses are based on an examination of low-resolution historical aerial photographs and would require confirmation through historical ground rephotography.

4.2. Modeling Natural Background and Urbanization-Related Erosion in the Metropolitan Phoenix Region

Figure 8 situates our estimates of background and urbanization-accelerated erosion in both spatially and temporally. Figure 8A displays the development history of the PMR, as shown in Figure 5. Figure 8B (Table S4, Supplementary File S2) presents our estimated background erosion rates for the entire PMR. A comparison with Figure 8A reveals that background erosion is typically higher in areas of the PMR that have been developed more recently and have historically been less urbanized. This is because background erosion tends to be higher in locations with steeper slopes, which are traditionally less favorable to construction and urbanization.

In contrast, Figure 8C shows that areas with lower background erosion rates tend to exhibit higher rates of urban-accelerated erosion. This is particularly evident in the central and earlier developed areas of the metropolitan region (see Figure 5). A likely explanation for this discrepancy is that the earliest phases of urbanization were concentrated in lower-lying, flatter areas, conditions that naturally favor lower rates of background erosion. Taken together, Figure 8B,C suggest that urbanization has the potential to accelerate erosion in areas that would otherwise be prone to low levels of background erosion, as well as in areas already experiencing higher levels of background erosion.

Figure 8D provides a temporal perspective by illustrating the annual urban growth rate (AUGR) and our estimate of urban-accelerated erosion in the PMR from 1912 to 2010. As expected, the acceleration of erosion by urbanization closely tracks the broader magnitude of urbanization over time. Prior to 1950, both urbanization and the erosion induced by urbanization were minimal. From the mid-1950s to 2000, both urbanization and erosion progressively increased decade by decade. The most striking increase in both metrics coincided with the widespread build of the early 2000s. These patterns of expansion and acceleration tapered off between 2005 and 2010, likely due to the slowdown in building and expansion following the USA's Great Recession. Erosion, and consequently soil sustainability, is closely linked to human development activities over time. Furthermore, erosion can occur in areas that deviate from typical background spatial patterns, highlighting the influence of urbanization on soil processes.

Figure 9 integrates our perspectives of time and space, as well as the interplay between natural background and urbanization-accelerated erosion processes. Figure 9A presents our estimates of the UAEN, indicating the degree to which urbanization accelerated the natural erosion process across the twentieth century.

A UAEN of "1" indicates that the level of erosion attributable to urbanization is equivalent to the level of natural background erosion. From 1912 to 1955, the UAEN ranged between 2.4 and 3.5, suggesting that urbanization during this period accelerated erosion by no more than 3.5 times the natural background rate. This acceleration increased significantly in subsequent decades, peaking during the 1985–1990 period, when urbanization accelerated erosion by approximately 23 times the background. The period following 1985 witnessed significant construction in the southeastern (e.g., Tempe, Gilbert, Chandler) and northwestern (e.g., Peoria) region of the PMR (see Figure 9B). Despite slight declining since the 1985–1990 peak, UAEN has remained high in the PMR.

Table 2 presents the transitions of UAE, background erosion, and UAEN in PMR from 1912 to 2010, derived from regression analysis. Sediment yield estimates from the bare ground layers exposed by urban expansion in PMR from 1912 to 2010 were $9 \text{ Mg km}^{-2} \text{ yr}^{-1}$ for background erosion and $111 \text{ Mg km}^{-2} \text{ yr}^{-1}$ for UAE. This analysis reveals an acceleration of soil erosion by a factor of 12.2 times above the natural background rate as Phoenix expanded over a century (Table 2).

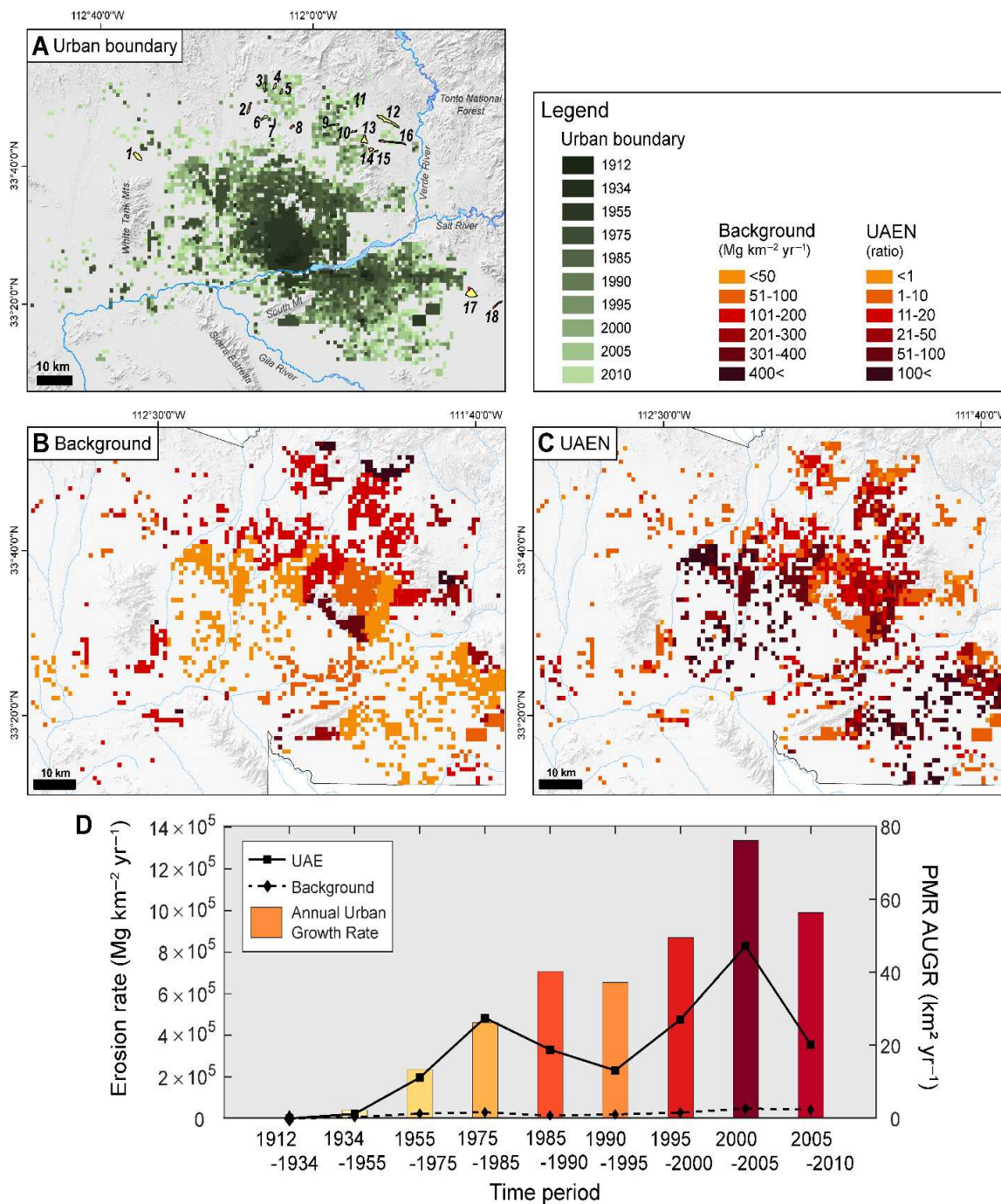


Figure 8. Spatial and temporal variability in natural and urbanization-generated soil erosion for metropolitan Phoenix, USA. (A) Urban sprawl of Phoenix metropolitan region from 1912 to 2010. (B) Spatial distribution of the modeled background erosion rate using CADR measurements, and (C) UAEN. (D) Temporal change in background erosion and UAE in PMR from 1912 to 2010 associated with PMR’s annual urban growth rate.

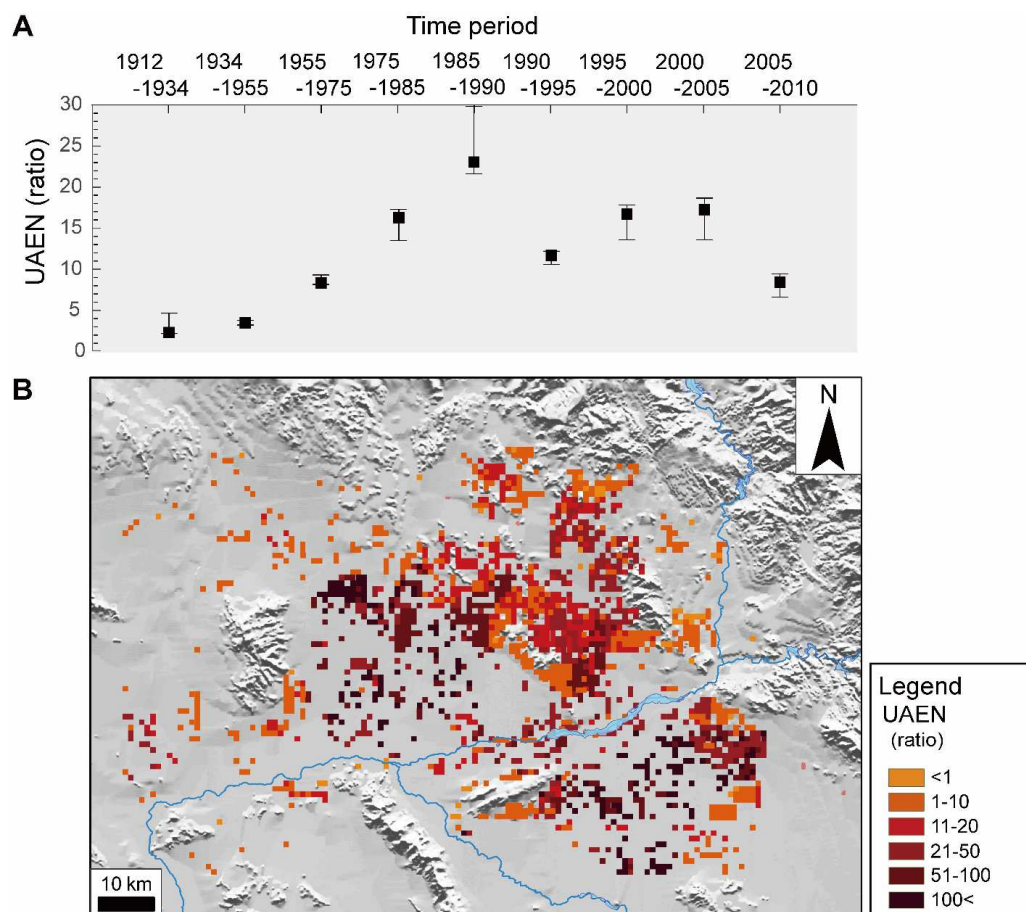


Figure 9. (A) Temporal change in the urban acceleration of erosion above natural background (UAEN) in PMR from 1912 to 2010. (B) Spatial distribution of the UAEN.

Table 2. Transition of UAE, background erosion, and UAEN in PMR from 1912 to 2010 derived from regression analyses.

Time Period	LT ¹ (yr)	ABG ² (km ²)	AUGR ³ (km ² yr ⁻¹)	Background ± 1σ (Mg)	UAE ± 1σ (Mg)	Background ± 1σ (Mg km ⁻² yr ⁻¹)	UAE ± 1σ (Mg km ⁻² yr ⁻¹)	UAEN ⁴ Mean	(-1σ)	(+1σ)
T1: 1912–1934	22	0.46	0.02	503 ± 404	1219 ± 789	49 ± 40	119 ± 77	2.4	2.2	4.3
T2: 1934–1955	21	44.81	2.13	10,318 ± 51,516	459,435 ± 208,082	138 ± 55	488 ± 221	3.5	3.2	3.7
T3: 1955–1975	20	266.79	13.34	468,878 ± 250,184	3,925,647 ± 1,916,566	88 ± 47	736 ± 359	8.4	8.1	9.2
T4: 1975–1985	10	262.39	26.24	296,872 ± 131,363	4,838,963 ± 2,589,339	113 ± 50	1844 ± 987	16.3	13.6	17.3
T5: 1985–1990	5	200.89	40.18	71,732 ± 45,628	1,655,341 ± 878,108	71 ± 45	1648 ± 874	23.1	21.6	29.8
T6: 1990–1995	5	186.06	37.21	98,353 ± 45,885	1,156,408 ± 596,934	106 ± 49	1243 ± 642	11.8	10.7	12.2
T7: 1995–2000	5	247.13	49.43	142,376 ± 61,607	2,377,551 ± 1,273,757	115 ± 50	1924 ± 1031	16.7	13.7	17.9
T8: 2000–2005	5	380.37	76.07	240,941 ± 99,622	4,147,279 ± 2,235,257	127 ± 52	2181 ± 1175	17.2	13.5	18.7
T9: 2005–2010	5	281.70	56.34	211,366 ± 79,733	1,779,401 ± 916,481	150 ± 57	1263 ± 651	8.4	6.6	9.3
T1–T9: 1912–2010	98	1870.61	19.09	1,661,338 ± 765,942	20,341,242 ± 10,615,315	9 ± 4	111 ± 58	12.2	10.9	12.8

¹ LT: length of time period. ² ABG: area of exposed bare ground during urbanization. ³ AUGR: annual urban growth rate calculated as ABG/the length of time period. ⁴ UAEN: urban acceleration of erosion above natural background erosion calculated as UAE/background.

4.3. Urban Cycle of Erosion for Arid Environments

The rocky desert landscape of the Phoenix, Arizona, USA, region exhibits significant sensitivity to soil erosion resulting from anthropogenic disturbance [22,52] (Table S2 in Supplementary File S4 and Figure 10). A comparison of sediment yields from the 1st and 3rd quartiles of each major LULCC category for the PMR reveals the following trends: (i) grazing increased sediment yields typically 0.5 to 6.6 times the natural background rates; (ii) human-set wildfires [53] elevated sediment yields by a factor of 1.9 to 10.6 times the natural background rates; (iii) the exposure of bare ground due to residential and commercial development resulted in sediment yields 7.5 to 61.8 times higher than natural background rates; and (iv) the sealing of urban surfaces led to sediment yields ranging from one-tenth to one-half of those associated with natural background erosion rates.

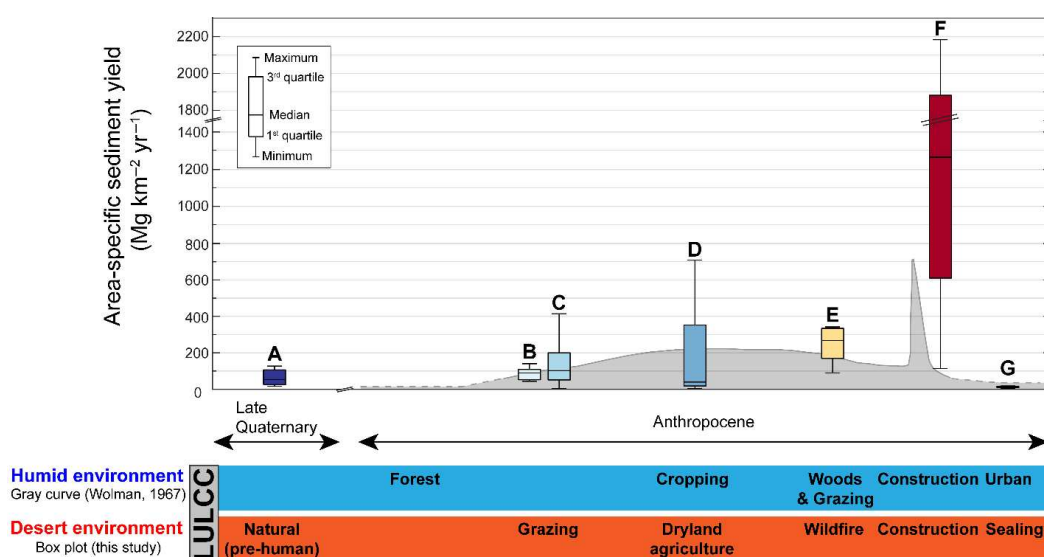


Figure 10. Box and whisker plots of area-specific sediment yield associated with LULCC in a warm desert environment compared with the humid-region prior model. The gray curve presents the classic cycle of land use change and sediment yield behavior developed for LULCC in Maryland [15]. Dashed lines in the gray curve indicate unmeasured but predicted lower erosion due to urban sealing effect [15]. Letters (A–G) correspond to different land uses associated LULCC in the PMR, with their associated area-specific sediment yield (SSY) data. Specific land use categories and associated sediment yields: (A) Background sediment yield: Derived from CADR from stock ponds in the PMR using ¹⁰Be [21]. (B) Grazing Period SSY: Collected from stock ponds in PMR during grazing period [22]. (C) Published grazing SSY: Collected from published grazing data in BWh catchments [22,51]. (D) Dryland agriculture SSY: Collected from published data from BWh catchments experiencing dryland agriculture [22,51]. (E) Wildfire SSY: Collected from stock ponds in PMR after wildfires [22]. (F) Construction period SSY: Estimated from our model for entire PMR from 1912 to 2010. (G) Urban sealing SSY: From the PMR in stock pond and other watersheds after urbanization sealed surfaces.

5. Discussion

The methods (Section 3) and Results Section (Section 4) provides detail about the observations and modeling used to obtain a first broad quantification of just how much urban growth accelerates soil erosion. It is crucial to acknowledge, however, that the models for estimating UAEN presented here are largely based on indirect comparisons across diverse catchments and data sources. Given these inherent limitations in data availability and modeling detail, there are also limits to their interpretation and, importantly, their transferability and general applicability to other regions. For example, this initial estimate suggests a potential climatic inflection point around 1500 mm of mean annual precipitation

(Figure 7), where the acceleration rate appears to change significantly. However, the rough nature of our modeling efforts, coupled with the limited dataset, renders it inappropriate to model how global changes might alter broader patterns of soil erosion, or to establish a rigid threshold. Indeed, the UAEN concept, while promising, remains insufficiently validated by independent data outside our Phoenix case study, especially for more humid climatic regions (MAP > 1500 mm) where output variability is considerable (ranging from 23× to 72×). This underscores a key limitation of our current model and the need for further verification. Therefore, despite our broader interest in global change, we focus this discussion on local applications for urban planners. We have sufficient confidence in the direction and approximate magnitude of soil erosion acceleration to recommend these findings for effective erosion management in urban contexts. Future research must explicitly address the degree of uncertainty, the model's limiting assumptions, and potential biases that may arise when transferring this model to regions with substantially different climatic, hydrological, and urbanization characteristics.

5.1. Sustainable Landscape Pattern and Urban Soil Sustainability

The provision of ecosystem services by soils makes their preservation a critical consideration in urban planning [10]. Widely recognized improvements to the urban environment include replacing impervious land surfaces with healthy soils and green groundcover and trees [54,55]. Thus, soil erosion, especially its potential for off-site movement and subsequent impacts, has emerged as a key concern in urban planning [55]. It is often the downstream consequences, such as degraded water quality or increased flood risks from transported sediment, that underline this significance.

It is important to recognize that the value and challenges of urban soils differ significantly from natural or agricultural contexts. While the ecological functions of urban soils are paramount, their perceived importance in planning can also be influenced by esthetic considerations, perceived quality of life in urban gardens and farms, or even the practical ability of clients or developers to import or 'manufacture' soil for specific purposes. Therefore, urban soil management often involves a more balanced view of soil dynamics, where the focus shifts from preventing all erosion to effectively managing its undesirable consequences.

Soil erosion is the opposite of soil retention—an important conservation priority for urban ecological land [56] (p. 3). Achieving sustainable landscape pattern (SLP) in cities requires soil retention [2] in order to carry out such activities as sustainable urban agriculture and urban greening [57] and associated resilience to urban heat islands [20]. Some argue that the carbon-storing function of urban soils could play a role in helping to control anthropogenic global warming [5]. Recognition of the importance of urban soils prompted a variety of soil-related sustainability strategies, including the artificial creation of soil [58], the unsealing of soils [59], or focusing more on natural soils that survived the urban sealing processes [59]. Irrespective of the scholar's preferred sustainability strategy, urban soils provide a wide variety of ecosystem services that are vital to sustaining our cities into the future [60–62]. Therefore, in the context of sustainable development, we hope to help spatial planners explore this practical dimension of SLP [49].

Specifically for spatial planning, natural background rates of soil erosion as measured by ^{10}Be CADR provide a useful "planning target" (cf. [49], p. 37) for sustainable rates of soil erosion. This is because soils maintain a dynamic equilibrium when rates of soil formation are equal to natural erosion rates [63]. Thus, the urban acceleration of erosion above natural background of 1 or below permits soil retention [64]. The overwhelmingly clear finding of this research is that all modeled global cities had urban accelerations above natural background rates of erosion (UAEN) much higher than 1 (Figure 7), including our

focused study region of metropolitan Phoenix (Figure 8). Historic rates of urban soil erosion greatly exceed rates of soil formation. In other words, no modeled or directly observed city had sustainable urban soils, because all analyzed cities experienced an anthropogenic acceleration of physical soil erosion far above natural values.

One piece of this sustainable future involves the post-industrial trend of urban agriculture efforts that enhance the sustainability of cities of the future [65]. Urban agriculture is part of urban greening [66], a way to cool cities [67] and better air quality [68]. Urban greening is also a nature-based strategy to mitigate the impact of urban flooding on urban soils [69]. Our basic finding of a non-sustainable UAEN much higher than 1 (Figures 7 and 8) does not directly influence the resilience of the remaining urban soils; shocks to soil health are an entirely different issue, typically involving such issues as heavy metal pollution or removal of organic carbon [70].

5.2. Testing Global Cities Model with Phoenix-Region Case Study

The largest problem with our global cities UAEN model is that there is no “apples to apples” comparison of the same watersheds studied for urbanization impacts and natural erosion rates. All of the natural rates we have available to compare with urbanization’s impact derive from the proxies of nearby drainages or samples collected from a similar climate region, introducing inherent uncertainty in these broader estimates. Thus, our detailed case study for the PMR, Arizona, USA (Figures 7–10) provides the first “apples to apples” comparison that we use to test the general accuracy of the global cities modeling results (Figure 7). While this case study strengthens our confidence, it also highlights the critical need for similar direct validation in other diverse urban settings to enhance the model’s robustness and transferability.

Our Phoenix case study reveals a ~12.2x acceleration of erosion; this resides in the middle of 7x–19x for drier global cities (Table 1; Figure 7). The natural question to ask is whether Phoenix is truly representative of an arid region in terms of its erosion rates and in terms of its soil production. Prior scholarship [71] does indicate that arid-region soil production is about the same as the long-term erosion rates we modeled for the Phoenix region (Figure 7).

This means that the next test of our approach to modeling the acceleration of soil erosion above sustainable natural background values should come from wetter global cities above 1500 mm precipitation with a UAEN envelope of 23x–72x (Figure 7). While it is beyond the scope of this study to replicate our Phoenix-region results for another urban area, our next step is to obtain samples from urbanizing watersheds on the perimeter of wetter cities (e.g., Table 1) for CADR analysis. Such a study would provide enhanced confidence that CADR offers clear “targets” for sustainable rates of urban soil erosion.

5.3. Spatial and Temporal Variability in Soil Sustainability

Our strategy to model soil erosion across the history of the metropolitan region of Phoenix reflects what Dong et al. [49] refer to as “frontier theory” supporting SLP development. While there is growing recognition that the field of urban sustainability lacks a firm scientific foundation for understanding critical sustainability processes [72] over the long durée, soils are particularly challenging, as their relevant spatial scale for analysis is often extremely fine. The construction of structures and roads can have an impact on the health of proximate soils. Our analysis therefore complements other recent sustainability research by integrating settlement and environmental data over long periods of time and at high spatial resolution within a land-based perspective [73].

The overall picture that we present suggests that the PMR lacks sustainable soils. This regional conclusion, however, may not be accurate for all places or times. The Phoenix-wide

modeling results presented here (Figure 8) indicates that there are periods of time and locations where urbanization's impact on soil erosion is less severe (e.g., UAEN < 1 in Figure 8C,D). For example, the Phoenix region experienced sustainable soil erosion prior to about 1975 (Figure 8C) and also in developments on lower slopes (Figure 8B).

Certainly, the spotty nature of Phoenix's sustainable soil erosion seen in Figure 8B,C might not be a pattern observed in other cities. However, the trend over time (Figure 8D) towards greater offsets between sustainable rates of soil erosion and urbanization's impact might be similar to other urban areas that are expanding their perimeter out towards steeper slopes. What our Phoenix model offers to other cities is the ability to model where accelerated soil erosion might occur and enhance efforts to mitigate this erosion. The mitigation might be as simple as allowing the growth of some vegetation cover [74,75] or not exposing piles of bare ground during a rainy season [76–78].

5.4. Why Precipitation Falling on Urban Construction Sites Is Different from Natural Watersheds: Implication for SLP Serving Spatial Planning

Our research on urban soil erosion operates within the “frontier theory” in Sustainable Landscape Planning (SLP), which necessitates placing soil erosion in a broader theoretical context [49]. For over six decades, the scientific discipline of geomorphology has debated the precise impact of precipitation on natural rates of soil erosion [79–82]. A prominent perspective from this debate is the model by Langbein and Schumm [83], which posited a skewed distribution of erosion rates with climate—specifically, lower rates in arid regions, maximum rates in semi-arid environments, and a subsequent decline in wetter places attributed to increased vegetation cover. However, this view is not universally accepted, as many studies in non-urban and non-agricultural settings show a low correlation between precipitation and erosion, largely due to the mitigating role of dense vegetation cover [79–81].

Our global cities modeling results, however, present a strong and distinct precipitation signal in urban environments, often characterized by a step function where erosion rates double or triple above ~1500 mm of mean annual precipitation (Figure 7 and Table 2). This striking contrast to natural settings reignites aspects of the long-standing debate within a new urban context, and is likely attributable to the widespread exposure of bare ground during urban construction. Unlike natural landscapes where vegetation acts as a primary buffer [79–81], urban construction processes frequently remove this protective cover entirely. In such disturbed urban settings, the basic drivers of erosion—rainfall intensity, surface runoff, and the inherent energy from slope—become dominant.

Specifically, the pronounced increase in erosion above 1500 mm precipitation can be explained by the fundamental process of rainsplash. While initial surface crusts can form on newly exposed bare ground and offer some temporary protection [84], the constant intensity and cumulative volume of precipitation typical of rainy seasons in wetter cities likely overwhelm this natural soil-crusting effect. Without the robust protection of vegetation, it is geomorphologically plausible that erosion rates would accelerate significantly once the limited protective capacity of soil crusting is exceeded by abundant rainfall.

This analysis underscores a critical point for spatial planning solutions to manage urban soil erosion problems and promote SLP. For example, construction projects can be strategically planned to expose bare ground predominantly during dry seasons, while carrying out other activities during wet periods. Another effective strategy is to protect soil piles under covers for their later use in urban agriculture or greening, after testing for lead and other contaminants [85]. Such solutions may seem obvious in retrospect and are easier to propose than to implement.

5.5. *The Urban Cycle of Erosion and Soil Sustainability*

The U.S. National Science Foundation supports long term ecological research (LTER) in two urban regions of the USA: Baltimore/Washington D.C. Maryland metropolitan region [25] and the Phoenix metropolitan area [24]. Wolman [15] proposed an urban cycle of erosion for the Baltimore/Washington D.C. area (Figure 1). We reinterpret here Wolman's broader thinking now in terms of SLP for more settings than Wolman's Baltimore/Washington D.C. setting.

The various spatial patterns of erosion across urban growth boundaries are space and time transgressive, something we were able to assess for the PMR. Thus, Wolman's general model can be interpreted in terms of urban soil sustainability (Figure 10). The Sonoran Desert setting of PMR experienced a sequence of LULCC different than the Maryland piedmont (Figure 10). Late Quaternary conditions in the PMR had low rates of soil erosion. Then, instead of deforestation, the studied watersheds underwent a period of grazing slightly increasing erosion above natural background rates. While the Phoenix area did have both prehistoric and historic agriculture [86], no data exists on soil erosion for either period. Thus, we plot global dryland agricultural data [22,51] for illustrative and comparative purposes. The PMR watersheds then experienced a spike in erosion from human-set wildfires [53] on the urban fringe [22]. Then, the largest effect on soil erosion came from a century of urbanization, as predicted in Wolman's model [15]. Soil erosion in the PMR then returned close to natural background levels after paving these urban surfaces.

Thus, both of the LTER urban areas of the USA National Science Foundation went through a long phase of accelerated soil erosion related to LULCC preceding urbanization. Both LTER urban areas experienced a massive spike in elevated urban soil erosion associated with construction. However, what we learned in the case of PMR, the ¹⁰Be CADR method offers a target for urban planning; hence we were able to quantify exactly how much enhancement occurred from such processes as grazing and wildfire that preceded urbanization (Figure 10) and that urban sealing drops soil erosion below natural CADR-quantified erosion rates.

5.6. *Broader Impacts of Urban Soil Erosion for Urban Planning*

It is important to highlight issues that extend beyond our focus on sustainable soils [2], given their significance for urban planning and SLP. Figure 2 in Dong et al. [49] present a ternary theoretical basis of a SLP. One leg of Dong et al.'s [49] ternary diagram involves a feedback loop between biodiversity and ecosystem processes. In the context of urban patterns, we view this ternary leg as truly involving soils. Consider the importance of soils as key to urban agriculture as part of urban greening [57], cooling cities [67], and aiding air quality [68]—especially in the global urban south that is a key for global sustainability [87].

We acknowledge that the rate, manner, and regulatory frameworks of urbanization vary significantly across the globe. This includes diverse approaches to managing and mitigating environmental impacts, such as 'biodiversity offsetting,' a mechanism through which urban development's impact on green open space assets is counterbalanced by their creation or enhancement elsewhere [88]. For instance, in Germany, particularly in cities like Berlin, urban development projects often include requirements for developers to provide compensation for environmental benefits or mitigate negative landscape impacts, formalized through mechanisms like eco-accounts [89]. Similarly, in the UK, specifically London, such compensation is facilitated through instruments like Section 106 agreements [88]. Beyond Europe, countries like the USA also have established requirements for mitigation and compensation, prominently for wetland losses, often involving concepts such as wetland mitigation banking. Other nations like the Netherlands and Sweden have also implemented various forms of environmental compensation within their planning sys-

tems, showcasing a diversity of approaches adapted to different legal and environmental contexts globally [90]. These varied policy measures underscore a global trend towards acknowledging and attempting to compensate for the environmental costs of urban growth.

The stakes associated with urbanization-enhanced soil erosion tend to be spatially variable, as tends to be for all soil erosion [60,91–93]. Beyond direct erosion impacts, urbanization fundamentally alters natural hydrology through increased impervious surfaces and modified drainage systems. This altered hydrology, in conjunction with soil erosion, leads to significant impacts on water quality. Involving SLP to help aid in urban planning (cf. [49]) naturally incorporates issues such as urban soil erosion impacting reservoirs [35], degraded water quality [94–96] and related health effects from heavy metals [97,98]. This is particularly critical as once urbanized areas stabilize, concerns may shift from soil quality itself to the overarching implications for water resources.

Moving forward into the twenty-first century demands that “urban sustainability, urban resilience and urban transformation” involves Earth System dynamics [99], such as soil erosion processes. These processes can also cause other urban sustainability complications such as eutrophication of freshwater systems due to the increased delivery of sediment containing P and N from fertilizers [100,101]. Soil erosion also impacts urban poverty in a variety of ways [102], including negative health impacts [103] and compromised water quality [104]. Enhanced urban soil erosion might remove carbon stored in city soils [5,105], or it might end up in a setting where it can be more stable such as a reservoir [106].

6. Conclusions

Our research on how urbanization accelerates soil erosion links to this Special Issue on land systems pertaining to global change by presenting new observations and new models of urban soil erosion. For the first time, we provide a comparison of natural long-term rates of soil erosion obtained through cosmogenic nuclide ^{10}Be analysis with direct observations of urban soil erosion over a century. This unique dataset exists only for the city of Phoenix in the Sonoran Desert of North America, where urban expansion accelerated soil erosion by about 12x. Unfortunately, no cosmogenic nuclide ^{10}Be data exist for other cities across different global climates. Thus, we had to model existing ^{10}Be data, and this led to only being able to provide a broad estimate that cities with mean annual precipitation <1500 mm experienced soil erosion acceleration of ~7–19x, similar to Phoenix. A jump in urban acceleration of soil erosion occurred for cities with mean annual precipitation >1500 mm. The next step in this research requires obtaining new data on cosmogenic nuclide ^{10}Be for global cities in different climates, instead of using modeled data.

The loss of soils in urban landscapes remains an understudied topic in global change and with likely long-term consequences for ecosystem services derived from urban landscapes [107]. In this first insight into quantifying the offset between urban soil erosion and sustainable rates of erosion, we offer new research strategies for urban planners to better understand urban soil sustainability, as follows: (i) a way to obtain sustainable rates of soil erosion via measurement of ^{10}Be cosmogenic nuclides from watersheds before they undergo urbanization; (ii) how to estimate natural background rates of soil erosion if ^{10}Be cosmogenic nuclide analyses were not feasible; and (iii) a strategy to statistically model rates of soil erosion across an urban area. Furthermore, the combination of our approach coincides with the emergence of new data pertaining to long-term urbanization patterns (e.g., [108]). The list of urban areas in Table 1 that were beyond the scope of our research design would be ideal candidates for ^{10}Be measurements to provide a natural baseline and a basic target of sustainable rates of soil erosion to aid spatial planners in promoting sustainable soils for urban planning.

Supplementary Materials: The following supporting information can be downloaded at: <https://www.mdpi.com/article/10.3390/land14081590/s1>, Supplementary File S1. Slope map for global cities; Supplementary File S2. Detailed methods (e.g., [15,17,21,22,27–29,31,35,109–120]); Supplementary File S3. The change changes in land use, precipitation and erosion rates for each of the 18 stock ponds catchments (e.g., [21]); Supplementary File S4. Supplementary data for validation of Wolman (1967) model (e.g., [15,21,22,51]).

Author Contributions: Conceptualization, A.J., D.S.C. and R.I.D.; methodology, A.J., D.S.C., R.I.D. and Y.B.S.; validation, A.J., D.S.C. and R.I.D.; formal analysis, A.J., D.S.C. and R.I.D.; investigation, A.J., D.S.C., R.I.D. and Y.B.S.; data curation, A.J. and R.I.D.; writing—original draft preparation, A.J., D.S.C. and R.I.D.; writing—review and editing, A.J., D.S.C., R.I.D. and Y.B.S.; visualization, A.J.; supervision, R.I.D. All authors have read and agreed to the published version of the manuscript.

Funding: This research received no external funding.

Data Availability Statement: The original contributions presented in this study are included in the article. Further inquiries can be directed to the corresponding author.

Acknowledgments: We thank B.L. Turner II, T. Dunne, M.W. Schmeckle, I.J. Walker, and K. Seto for suggestions at different stages of manuscript preparation, and the School of Geographical Sciences & Urban Planning of Arizona State University for support.

Conflicts of Interest: The authors declare no conflicts of interest.

Abbreviations

The following abbreviations are used in this manuscript:

CADR	Catchment-averaged denudation rate
PMR	Phoenix Metropolitan Region
UAE	Urban-accelerated erosion
UAEN	Urbanization's acceleration of soil erosion above natural background
LULCC	Land use and land cover changes
SSY	Area-specific sediment yields
MAP	Mean annual precipitation
SLP	Sustainable landscape pattern

References

- De Kimpe, C.R.; Morel, J.L. Urban soil management: A growing concern. *Soil Sci.* **2000**, *165*, 31–40. [[CrossRef](#)]
- Kumar, K.; Hundal, L.S. Soil in the City: Sustainably Improving Urban Soils. *J. Environ. Qual.* **2016**, *45*, 2–8. [[CrossRef](#)]
- Louise, A.; Lucas, M.; Adrien, T.; Cyrille, V.; Franck, R. After-sealing life in urban soils: Experimental evidence of resilience and efficiency of ectomycorrhizal inoculation. *Landsc. Urban Plan.* **2024**, *251*, 105149. [[CrossRef](#)]
- Pouyat, R.V.; Yesilonis, I.D.; Nowak, D.J. Carbon Storage by Urban Soils in the United States. *J. Environ. Qual.* **2006**, *35*, 1566–1575. [[CrossRef](#)]
- Vasenev, V.; Kuzyakov, Y. Urban soils as hot spots of anthropogenic carbon accumulation: Review of stocks, mechanisms and driving factors. *Land Degrad. Dev.* **2018**, *29*, 1607–1622. [[CrossRef](#)]
- Johnston, M.R.; Balster, N.J.; Zhu, J. Impact of Residential Prairie Gardens on the Physical Properties of Urban Soil in Madison, Wisconsin. *J. Environ. Qual.* **2016**, *45*, 45–52. [[CrossRef](#)]
- Berland, A.; Shiflett, S.A.; Shuster, W.D.; Garmestani, A.S.; Goddard, H.C.; Herrmann, D.L.; Hopton, M.E. The role of trees in urban stormwater management. *Landsc. Urban Plan.* **2017**, *162*, 167–177. [[CrossRef](#)] [[PubMed](#)]
- Edmondson, J.L.; Stott, I.; Davies, Z.G.; Gaston, K.J.; Leake, J.R. Soil surface temperatures reveal moderation of the urban heat island effect by trees and shrubs. *Sci. Rep.* **2016**, *6*, 33708. [[CrossRef](#)]
- Murata, T.; Kawai, N. Degradation of the urban ecosystem function due to soil sealing: Involvement in the heat island phenomenon and hydrologic cycle in the Tokyo metropolitan area. *Soil Sci. Plant Nutr.* **2018**, *64*, 145–155. [[CrossRef](#)]
- da Silva, R.T.; Fleskens, L.; van Delden, H.; van der Ploeg, M. Incorporating soil ecosystem services into urban planning: Status, challenges and opportunities. *Landsc. Ecol.* **2018**, *33*, 1087–1102. [[CrossRef](#)]
- Anne, B.; Geoffroy, S.; Cherel, J.; Warot, G.; Marie, S.; Noël, C.J.; Louis, M.J.; Christophe, S. Towards an operational methodology to optimize ecosystem services provided by urban soils. *Landsc. Urban Plan.* **2018**, *176*, 1–9. [[CrossRef](#)]

12. Zhao, J.; Yu, L.; Zhao, L.; Fu, H.; Gong, P. Significant contribution of urban morphological diversity to urban surface thermal heterogeneity. *Urban Clim.* **2025**, *61*, 102383. [[CrossRef](#)]
13. Zou, Y.; Chen, W.; Li, S.; Wang, T.; Yu, L.; Zhang, X.; Xu, M.; Jiang, B.; Wu, C.; Singh, R.P.; et al. Assessing vegetation dynamics and human impacts in natural and urban areas of China: Insights from remote sensing data. *J. Environ. Manag.* **2025**, *373*, 123632. [[CrossRef](#)]
14. Zhao, J.; Chen, W.; Liu, Z.; Liu, W.; Li, K.; Zhang, B.; Yu, L.; Sakai, T. Urban expansion, economic development, and carbon emissions: Trends, patterns, and decoupling in mainland China's provincial capitals (1985–2020). *Ecol. Indic.* **2024**, *169*, 112777. [[CrossRef](#)]
15. Wolman, M. A cycle of sedimentation and erosion in urban river channels. *Geogr. Ann. Ser. A Phys. Geogr.* **1967**, *49*, 385–395. [[CrossRef](#)]
16. Shikangalah, R.N.; Jeltsch, F.; Blaum, N.; Mueller, E.N. A review on urban soil water erosion. *J. Stud. Humanit. Soc. Sci.* **2016**, *5*, 163–178.
17. Russell, K.L.; Vietz, G.J.; Fletcher, T.D. Global sediment yields from urban and urbanizing watersheds. *Earth-Sci. Rev.* **2017**, *168*, 73–80. [[CrossRef](#)]
18. von Blanckenburg, F. The control mechanisms of erosion and weathering at basin scale from cosmogenic nuclides in river sediment. *Earth Planet. Sci. Lett.* **2005**, *237*, 462–479. [[CrossRef](#)]
19. Talen, E. Zoning for and Against Sprawl: The Case for Form-Based Codes. *J. Urban Des.* **2013**, *18*, 175–200. [[CrossRef](#)]
20. Keith, L.; Meerow, S. Planning for urban heat resilience. In *Planning Advisory Services (PAS) Report*; American Planning Association: Chicago, IL, USA, 2011; Available online: <http://www.planning.org/publications/report/9245695/> (accessed on 31 July 2025).
21. Jeong, A.; Dorn, R.I.; Seong, Y.-B.; Yu, B.-Y. Acceleration of Soil Erosion by Different Land Uses in Arid Lands above ¹⁰Be Natural Background Rates: Case Study in the Sonoran Desert, USA. *Land* **2021**, *10*, 834. [[CrossRef](#)]
22. Jeong, A.; Dorn, R.I. Soil erosion from urbanization processes in the Sonoran Desert, Arizona, USA. *Land Degrad. Dev.* **2019**, *30*, 226–238. [[CrossRef](#)]
23. U.S. Census Bureau. City and Town Population Totals: 2020–2023. Available online: <https://www.census.gov/data/tables/time-series/demo/popest/2020s-total-cities-and-towns.html> (accessed on 31 July 2025).
24. Arizona State University. Central Arizona–Phoenix Long-Term Ecological Research. Available online: <https://sustainability-innovation.asu.edu/caplter/> (accessed on 31 July 2025).
25. LTER Network. Baltimore Ecosystem Study. Available online: <https://lternet.edu/site/baltimore-ecosystem-study/> (accessed on 31 July 2025).
26. Peng, J.; Stuhlmacher, M.; Georgescu, M.; Wang, M.; Turner, B., II. More agglomerations, more polarization? Urban development during the last 20 years in China. *Res. Sq.* **2022**, preprint. [[CrossRef](#)]
27. Reusser, L.; Bierman, P.; Rood, D. Quantifying human impacts on rates of erosion and sediment transport at a landscape scale. *Geology* **2015**, *43*, 171–174. [[CrossRef](#)]
28. Portenga, E.W.; Bierman, P.R.; Trodick, C.D., Jr.; Greene, S.E.; DeJong, B.D.; Rood, D.H.; Pavich, M.J. Erosion rates and sediment flux within the Potomac River basin quantified over millennial timescales using beryllium isotopes. *GSA Bull.* **2019**, *131*, 1295–1311. [[CrossRef](#)]
29. Harel, M.-A.; Mudd, S.; Attal, M. Global analysis of the stream power law parameters based on worldwide ¹⁰Be denudation rates. *Geomorphology* **2016**, *268*, 184–196. [[CrossRef](#)]
30. Fekete, B.M.; Vörösmarty, C.J.; Grabs, W. High-resolution fields of global runoff combining observed river discharge and simulated water balances. *Glob. Biogeochem. Cycles* **2002**, *16*, 10–15. [[CrossRef](#)]
31. Saiz, A. The geographic determinants of housing supply. *Q. J. Econ.* **2010**, *125*, 1253–1296. [[CrossRef](#)]
32. Furbish, D.J.; Hamner, K.K.; Schmeekle, M.; Borosund, M.N.; Mudd, S.M. Rain splash of dry sand revealed by high-speed imaging and sticky paper splash targets. *J. Geophys. Res. Earth Surf.* **2007**, *112*, F01001. [[CrossRef](#)]
33. Deinlein, R.; Böhm, A. *Modeling Overland Flow and Soil Erosion for a Military Training Area in Southern Germany BT—Soil Erosion: Application of Physically Based Models*; Schmidt, J., Ed.; Springer: Berlin/Heidelberg, Germany, 2000; pp. 163–178. [[CrossRef](#)]
34. Ferreira, C.S.S.; Ferreira, A.J.D.; Pato, R.L.; Magalhães, M.d.C.; Coelho, C.d.O.; Santos, C. Rainfall-runoff-erosion relationships study for different land uses, in a sub-urban area. *Z. Fur. Geomorphol.* **2012**, *56*, 5–20. [[CrossRef](#)]
35. Jeong, A. Sediment accumulation expectations for growing desert cities: A realistic desired outcome to be used in constructing appropriately sized sediment storage of flood control structures. *Environ. Res. Lett.* **2019**, *14*, 125005. [[CrossRef](#)]
36. Yao, F.; Wu, J.; Li, W.; Peng, J. Estimating daily PM_{2.5} concentrations in Beijing using 750-M VIIRS IP AOD retrievals and a nested spatiotemporal statistical model. *Remote. Sens.* **2019**, *11*, 841. [[CrossRef](#)]
37. Gellis, A.; Myers, M.; Noe, G.; Hupp, C.; Schenk, E.; Myers, L. Storms, channel changes, and a sediment budget for an urban-suburban stream, Difficult Run, Virginia, USA. *Geomorphology* **2017**, *278*, 128–148. [[CrossRef](#)]
38. Verstraeten, G.; Poesen, J. Variability of dry sediment bulk density between and within retention ponds and its impact on the calculation of sediment yields. *Earth Surf. Process. Landf.* **2001**, *26*, 375–394. [[CrossRef](#)]

39. Schaller, M.; von Blanckenburg, F.; Hovius, N.; Kubik, P. Large-scale erosion rates from in situ-produced cosmogenic nuclides in European river sediments. *Earth Planet. Sci. Lett.* **2001**, *188*, 441–458. [[CrossRef](#)]
40. Bierman, P.R.; Reuter, J.M.; Pavich, M.; Gellis, A.C.; Caffee, M.W.; Larsen, J. Using cosmogenic nuclides to contrast rates of erosion and sediment yield in a semi-arid, arroyo-dominated landscape, Rio Puerco Basin, New Mexico. *Earth Surf. Process. Landf.* **2005**, *30*, 935–953. [[CrossRef](#)]
41. Singh, G.; Panda, R.K. Grid-cell based assessment of soil erosion potential for identification of critical erosion prone areas using USLE, GIS and remote sensing: A case study in the Kappari watershed, India. *Int. Soil Water Conserv. Res.* **2017**, *5*, 202–211. [[CrossRef](#)]
42. Pham, T.G.; Degener, J.; Kappas, M. Integrated universal soil loss equation (USLE) and Geographical Information System (GIS) for soil erosion estimation in A Sap basin: Central Vietnam. *Int. Soil Water Conserv. Res.* **2018**, *6*, 99–110. [[CrossRef](#)]
43. Didoné, E.J.; Minella, J.P.G.; Picilli, D.G.A. How to model the effect of mechanical erosion control practices at a catchment scale? *Int. Soil Water Conserv. Res.* **2021**, *9*, 370–380. [[CrossRef](#)]
44. Gao, G.; Liang, Y.; Liu, J.; Dunkerley, D.; Fu, B. A modified RUSLE model to simulate soil erosion under different ecological restoration types in the loess hilly area. *Int. Soil Water Conserv. Res.* **2024**, *12*, 258–266. [[CrossRef](#)]
45. Aswathy, S.S.; Sindhu, P. Effect of urbanization on soil erosion. *Int. J. Innov. Res. Sci. Eng. Technol.* **2013**, *2*, 75–81.
46. Chicas, S.D.; Omine, K.; Ford, J.B. Identifying erosion hotspots and assessing communities' perspectives on the drivers, underlying causes and impacts of soil erosion in Toledo's Rio Grande Watershed: Belize. *Appl. Geogr.* **2016**, *68*, 57–67. [[CrossRef](#)]
47. Polovina, S.; Radić, B.; Ristić, R.; Kovačević, J.; Milčanović, V.; Živanović, N. Soil erosion assessment and prediction in urban landscapes: A new G2 model approach. *Appl. Sci.* **2021**, *11*, 4154. [[CrossRef](#)]
48. Wu, J.; Li, J.; Peng, J.; Li, W.; Xu, G.; Dong, C. Applying land use regression model to estimate spatial variation of PM2.5 in Beijing, China. *Environ. Sci. Pollut. Res.* **2015**, *22*, 7045–7061. [[CrossRef](#)]
49. Dong, J.; Jiang, H.; Gu, T.; Liu, Y.; Peng, J. Sustainable landscape pattern: A landscape approach to serving spatial planning. *Landsc. Ecol.* **2022**, *37*, 31–42. [[CrossRef](#)]
50. Wolman, M.G.; Schick, A.P. Effects of construction on fluvial sediment, urban and suburban areas of Maryland. *Water Resour. Res.* **1967**, *3*, 451–464. [[CrossRef](#)]
51. Vanmaercke, M.; Poesen, J.; Broeckx, J.; Nyssen, J. Sediment yield in Africa. *Earth-Sci. Rev.* **2014**, *136*, 350–368. [[CrossRef](#)]
52. Jeong, A.; Cheung, S.Y.; Walker, I.J.; Dorn, R.I. Urban Geomorphology of an Arid City: Case Study of Phoenix, Arizona. In *Urban Geomorphology Landforms and Processes in Cities*; Thornbush, M.J., Allen, C.D., Eds.; Elsevier: Amsterdam, The Netherlands, 2018; pp. 177–204. [[CrossRef](#)]
53. D'Antonio, C.M.; Vitousek, P.M. Biological Invasions by Exotic Grasses, the Grass/Fire Cycle, and Global Change. *Annu. Rev. Ecol. Syst.* **1992**, *23*, 63–87. [[CrossRef](#)]
54. Séré, G.; Le Guern, C.; Bispo, A.; Layet, C.; Ducommun, C.; Clesse, M.; Schwartz, C.; Vidal-Beaudet, L. Selection of soil health indicators for modelling soil functions to promote smart urban planning. *Sci. Total. Environ.* **2024**, *924*, 171347. [[CrossRef](#)]
55. Hutahaean, M.; Sagala, S.; Subrata, S.A.; Zawani, H.; Insan, A.; Noer, I.S.; Wijaya, H.; Putra, D.D. Sustainable Urban Planning through Green Belt in IKN: A Literature Review. *IOP Conf. Ser. Earth Environ. Sci.* **2025**, *1447*, 012030. [[CrossRef](#)]
56. Peng, J.; Wang, A.; Luo, L.; Liu, Y.; Li, H.; Hu, Y.; Meersmans, J.; Wu, J. Spatial identification of conservation priority areas for urban ecological land: An approach based on water ecosystem services. *Land Degrad. Dev.* **2019**, *30*, 683–694. [[CrossRef](#)]
57. Feng, D.; Bao, W.; Yang, Y.; Fu, M. How do government policies promote greening? Evidence from China. *Land Use Policy* **2021**, *104*, 105389. [[CrossRef](#)]
58. Cannavo, P.; Vidal-Beaudet, L.; Grosbellet, C. Prediction of long-term sustainability of constructed urban soil: Impact of high amounts of organic matter on soil physical properties and water transfer. *Soil Use Manag.* **2014**, *30*, 272–284. [[CrossRef](#)]
59. Maienza, A.; Ungaro, F.; Baronti, S.; Colzi, I.; Giagnoni, L.; Gonnelli, C.; Renella, G.; Ugolini, F.; Calzolari, C. Biological Restoration of Urban Soils after De-Sealing Interventions. *Agriculture* **2021**, *11*, 190. [[CrossRef](#)]
60. Shikangalah, R.N. Soil loss estimation in a semi-arid mountainous catchment environment, City of Windhoek, Namibia. *J. Stud. Humanit. Soc. Sci.* **2017**, *6*, 209–222.
61. O'Riordan, R.; Davies, J.; Stevens, C.; Quinton, J.N.; Boyko, C. The ecosystem services of urban soils: A review. *Geoderma* **2021**, *395*, 115076. [[CrossRef](#)]
62. Xu, Z.; Peng, J.; Zhang, H.; Liu, Y.; Dong, J.; Qiu, S. Exploring spatial correlations between ecosystem services and sustainable development goals: A regional-scale study from China. *Landsc. Ecol.* **2022**, *37*, 3201–3221. [[CrossRef](#)]
63. Heimsath, A.M.; Dietrich, W.E.; Nishiizumi, K.; Finkel, R.C. The soil production function and landscape equilibrium. *Nature* **1997**, *388*, 358–361. [[CrossRef](#)]
64. Verheijen, F.G.; Jones, R.J.; Rickson, R.J.; Smith, C.J. Tolerable versus actual soil erosion rates in Europe. *Earth-Sci. Rev.* **2009**, *94*, 23–38. [[CrossRef](#)]
65. Palmer, L. Urban agriculture growth in US cities. *Nat. Sustain.* **2018**, *1*, 5–7. [[CrossRef](#)]

66. Thornbush, M. Urban agriculture in the transition to low carbon cities through urban greening. *AIMS Environ. Sci.* **2015**, *2*, 852–867. [[CrossRef](#)]
67. Bowler, D.E.; Buyung-Ali, L.; Knight, T.M.; Pullin, A.S. Urban greening to cool towns and cities: A systematic review of the empirical evidence. *Landsc. Urban Plan.* **2010**, *97*, 147–155. [[CrossRef](#)]
68. Pereira, P.; Inácio, M.; Karnauskaitė, D.; Bogdzevič, K.; Gomes, E.; Kalinauskas, M.; Barcelo, D. Nature-Based Solutions Impact on Urban Environment Chemistry: Air, Soil, and Water. In *The Handbook of Environmental Chemistry*; Barceló, D., Kostianoy, A.G., Eds.; Springer: Berlin/Heidelberg, Germany, 2021; pp. 1–59. [[CrossRef](#)]
69. Jakubínský, J.; Pechanec, V.; Cudlín, O.; Purkyt, J.; Cudlín, P. Identification of Surface Runoff Source Areas as a Tool for Projections of NBS in Water Management. In *The Handbook of Environmental Chemistry*; Barceló, D., Kostianoy, A.G., Eds.; Springer: Berlin/Heidelberg, Germany, 2021; pp. 1–26. [[CrossRef](#)]
70. Seybold, C.A.; Herrick, J.E.; Brejda, J.J. Soil resilience: A fundamental component of soil quality. *Soil Sci.* **1999**, *164*, 224–234. [[CrossRef](#)]
71. Stockmann, U.; Minasny, B.; McBratney, A.B. How fast does soil grow? *Geoderma* **2014**, *216*, 48–61. [[CrossRef](#)]
72. Smith, M.E.; Lobo, J.; Peeples, M.A.; York, A.M.; Stanley, B.W.; Crawford, K.A.; Gauthier, N.; Huster, A.C. The persistence of ancient settlements and urban sustainability. *Proc. Natl. Acad. Sci. USA* **2021**, *118*, e2018155118. [[CrossRef](#)]
73. Braswell, A.E.; Leyk, S.; Connor, D.S.; Uhl, J.H. Creeping disaster along the U.S. coastline: Understanding exposure to sea level rise and hurricanes through historical development. *PLoS ONE* **2022**, *17*, e0269741. [[CrossRef](#)]
74. Morrow, S.; Smolen, M.; Stiegler, J.; Cole, J.; Protection, T.; Using Vegetation for Erosion Control on Construction Sites. Oklahoma Cooperative Extension Service BAE-1514. 2003. Available online: <http://pods.dasnr.okstate.edu/docushare/dsweb/Get/Document-2264/BAE-1514web.pdf> (accessed on 31 July 2025).
75. Adewuyi, T.O.; Olofin, E.A.; Olutunmogun, A.K. Examination of the relationship between vegetation cover indices and land degradation in the peri-urban area of Kaduna metropolis, Nigeria. *J. Res. For. Wildl. Environ.* **2017**, *9*, 50–60.
76. Chen, X.; Huang, Y.; Gong, X. The Related Problems in the Construction of the Rainy Season. *Reg.—Water Conserv.* **2017**, *1*, 33–41. [[CrossRef](#)]
77. Matsukuma, S.; Sato, S.; Fuubayashi, Y. Demonstration of road improvement by local inhabitants at the Baytsemal Village in the South Omo Zone in southern Ethiopia. *Zairaiichi* **2020**, *3*, 1–23. [[CrossRef](#)]
78. Liu, L.; Zheng, J.; Guan, J.; Han, W.; Liu, Y. Grassland cover dynamics and their relationship with climatic factors in China from 1982 to 2021. *Sci. Total. Environ.* **2023**, *905*, 167067. [[CrossRef](#)] [[PubMed](#)]
79. Riebe, C.S.; Kirchner, J.W.; Granger, D.E.; Finkel, R.C. Minimal climatic control on erosion rates in the Sierra Nevada, California. *Geology* **2001**, *29*, 447–450. [[CrossRef](#)]
80. Reiners, P.W.; Ehlers, T.A.; Mitchell, S.G.; Montgomery, D.R. Coupled spatial variations in precipitation and long-term erosion rates across the Washington Cascades. *Nature* **2003**, *426*, 645–647. [[CrossRef](#)]
81. Mishra, A.K.; Placzek, C.; Jones, R.; Zerboni, A. Coupled influence of precipitation and vegetation on millennial-scale erosion rates derived from ¹⁰Be. *PLoS ONE* **2019**, *14*, e0211325. [[CrossRef](#)]
82. Jeong, A.; Seong, Y.B.; Dorn, R.I.; Yu, B.Y. Precipitation as a key control on erosion rates in the tectonically inactive northeastern Sonoran Desert, central Arizona, USA. *Phys. Geogr.* **2024**, *45*, 53–83. [[CrossRef](#)]
83. Langbein, W.B.; Schumm, S.A. Yield of sediment in relation to mean annual precipitation. *Trans. Am. Geophys. Union* **1958**, *39*, 1076–1084. [[CrossRef](#)]
84. Epstein, E.; Grant, W.J. *Soil Crust Formation as Affected by Raindrop Impact BT—Physical Aspects of Soil Water and Salts in Ecosystems*; Hadas, A., Swartzendruber, D., Rijtema, P.E., Fuchs, M., Yaron, B., Eds.; Springer: Berlin/Heidelberg, Germany, 1973; pp. 195–201. [[CrossRef](#)]
85. Laidlaw, M.A.; Filippelli, G.M.; Brown, S.; Paz-Ferreiro, J.; Reichman, S.M.; Netherway, P.; Truskewycz, A.; Ball, A.S.; Mielke, H.W. Case studies and evidence-based approaches to addressing urban soil lead contamination. *Appl. Geochem.* **2017**, *83*, 14–30. [[CrossRef](#)]
86. Rice, G.E. *Sending the Spirits Home: The Archaeology of Hohokam Mortuary Practices*; University of Utah Press: Salt Lake City, UT, USA, 2015. [[CrossRef](#)]
87. Nagendra, H.; Bai, X.; Brondizio, E.S.; Lwasa, S. The urban south and the predicament of global sustainability. *Nat. Sustain.* **2018**, *1*, 341–349. [[CrossRef](#)]
88. Danneels, K. Compensation landscapes. *Landsc. Res.* **2024**, 1–12. [[CrossRef](#)]
89. Baganz, G.F.M.; Baganz, D. Compensating for loss of nature and landscape in a growing city—Berlin case study. *Land* **2023**, *12*, 567. [[CrossRef](#)]
90. Rundcrantz, K.; Skärbäck, E. Environmental compensation in planning: A review of five different countries with major emphasis on the German system. *Eur. Environ.* **2003**, *13*, 204–226. [[CrossRef](#)]
91. Vanmaercke, M.; Poesen, J.; Govers, G.; Verstraeten, G. Quantifying human impacts on catchment sediment yield: A continental approach. *Glob. Planet. Chang.* **2015**, *130*, 22–36. [[CrossRef](#)]

92. Borrelli, P.; Robinson, D.A.; Fleischer, L.R.; Lugato, E.; Ballabio, C.; Alewell, C.; Meusburger, K.; Modugno, S.; Schütt, B.; Ferro, V.; et al. An assessment of the global impact of 21st century land use change on soil erosion. *Nat. Commun.* **2017**, *8*, 2013. [[CrossRef](#)]
93. Poesen, J. Soil erosion in the Anthropocene: Research needs. *Earth Surf. Process. Landf.* **2018**, *43*, 64–84. [[CrossRef](#)]
94. Baker, D.L.; King, K.A. *Environmental Contaminant Investigation of Water Quality, Sediment and Biota of the Upper Gila Riever Basin, Arizona*; US Fish and Wildfire Service: Washington, DC, USA; Arizona Ecological Services Field Office: Phoenix, AZ, USA, 1994. Available online: <https://azmemory.azlibrary.gov/nodes/view/207618> (accessed on 31 July 2025).
95. Issaka, S.; Ashraf, M.A. Impact of soil erosion and degradation on water quality: A review. *Geol. Ecol. Landsc.* **2017**, *1*, 1–11. [[CrossRef](#)]
96. Liu, G.; Zhang, Y.; Knibbe, W.-J.; Feng, C.; Liu, W.; Medema, G.; van der Meer, W. Potential impacts of changing supply-water quality on drinking water distribution: A review. *Water Res.* **2017**, *116*, 135–148. [[CrossRef](#)] [[PubMed](#)]
97. Zhuo, X.; Boone, C.G.; Shock, E.L. Soil lead distribution and environmental justice in the phoenix metropolitan region. *Environ. Justice* **2012**, *5*, 206–213. [[CrossRef](#)]
98. Rickson, R.J. Can control of soil erosion mitigate water pollution by sediments? *Sci. Total. Environ.* **2014**, *468–469*, 1187–1197. [[CrossRef](#)] [[PubMed](#)]
99. Elmqvist, T.; Andersson, E.; Frantzeskaki, N.; McPhearson, T.; Olsson, P.; Gaffney, O.; Takeuchi, K.; Folke, C. Sustainability and resilience for transformation in the urban century. *Nat. Sustain.* **2019**, *2*, 267–273. [[CrossRef](#)]
100. Carpenter, S.R.; Bennett, E.M. Reconsideration of the planetary boundary for phosphorus. *Environ. Res. Lett.* **2011**, *6*, 014009. [[CrossRef](#)]
101. Steffen, W.; Richardson, K.; Rockström, J.; Cornell, S.E.; Fetzer, I.; Bennett, E.M.; Biggs, R.; Carpenter, S.R.; De Vries, W.; De Wit, C.A.; et al. Planetary boundaries: Guiding human development on a changing planet. *Science* **2015**, *347*, 1259855. [[CrossRef](#)]
102. Shikangalah, R.N.; Paton, E.N.; Jeltsch, F. An analysis of stakeholders' perceptions on urban water erosion in Windhoek, Namibia. *J. Stud. Humanit. Soc. Sci.* **2019**, *89*, 3–28.
103. Li, G.; Sun, G.-X.; Ren, Y.; Luo, X.-S.; Zhu, Y.-G. Urban soil and human health: A review. *Eur. J. Soil Sci.* **2018**, *69*, 196–215. [[CrossRef](#)]
104. Pribadi, D.O.; Vollmer, D.; Pauleit, S. Impact of peri-urban agriculture on runoff and soil erosion in the rapidly developing metropolitan area of Jakarta, Indonesia. *Reg. Environ. Chang.* **2018**, *18*, 2129–2143. [[CrossRef](#)]
105. Scharenbroch, B.; Day, S.; Trammell, T.; Pouyat, R. Urban soil carbon storage. In *Urban Soils*; CRC Press: Boca Raton, FL, USA, 2017; pp. 137–154. [[CrossRef](#)]
106. Sanderman, J.; Berhe, A.A. The soil carbon erosion paradox. *Nat. Clim. Chang.* **2017**, *7*, 317–319. [[CrossRef](#)]
107. Herrmann, D.L.; Schifman, L.A.; Shuster, W.D. Widespread loss of intermediate soil horizons in urban landscapes. *Proc. Natl. Acad. Sci. USA* **2018**, *115*, 6751–6755. [[CrossRef](#)]
108. Leyk, S.; Uhl, J.H.; Connor, D.S.; Braswell, A.E.; Mietkiewicz, N.; Balch, J.K.; Gutmann, M. Two centuries of settlement and urban development in the United States. *Sci. Adv.* **2020**, *6*, eaba2937. [[CrossRef](#)] [[PubMed](#)]
109. Arnhold, S.; Lindner, S.; Lee, B.; Martin, E.; Kettering, J.; Nguyen, T.T.; Koellner, T.; OK, Y.S.; Huwe, B. Conventional and organic farming: Soil erosion and conservation potential for row crop cultivation. *Geoderma* **2014**, *219*, 89–105. [[CrossRef](#)]
110. Balamurugan, G. Tin mining and sediment supply in peninsular malaysia with special reference to the Kelang River Basin. *Environmentalist* **1991**, *11*, 281–291. [[CrossRef](#)]
111. De Vente, J.; Poesen, J. Predicting soil erosion and sediment yield at the basin scale: Scale issues and semi-quantitative models. *Earth-Sci. Rev.* **2005**, *71*, 95–125. [[CrossRef](#)]
112. Fox, R.L. The urbanizing river: A case study in the Maryland Piedmont. In *Geomorphology and Engineering*; Coates, D.R., Ed.; Dowden, Hutchinson, and Ross, Inc.: Stroudsburg, PA, USA, 1976; pp. 245–271.
113. Kinoshita, T.; Yamazaki, Y. Increase of sediment transport due to large-scale urbanization. *IAHS Publ.* **1974**, *113*, 130–136.
114. Leh, M.; Bajwa, S.; Chaubey, I. Impact of land use change on erosion risk: An integrated remote sensing, geographic information system and modeling methodology. *Land Degrad. Dev.* **2013**, *24*, 409–421. [[CrossRef](#)]
115. Patowary, S.; Sarma, A.K. GIS-Based Estimation of Soil Loss from Hilly Urban Area Incorporating Hill Cut Factor into RUSLE. *Water Resour. Manage.* **2018**, *32*, 3535–3547. [[CrossRef](#)]
116. Pope, I.C.; Odhiambo, B.K. Soil erosion and sediment fluxes analysis: A watershed study of the Ni Reservoir, Spotsylvania County, VA, USA. *Environ. Monit. Assess.* **2014**, *186*, 1719–1733. [[CrossRef](#)] [[PubMed](#)]
117. Portenga, E.W.; Bierman, P.R. Understanding Earth's eroding surface with ¹⁰Be. *GSA Today* **2011**, *21*, 4–10. [[CrossRef](#)]
118. Sarma, A.K.; Chandramouli, V.; Singh, B.; Goswami, P.; Rajbongshi, N. Urban flood hazard mitigation of Guwahati city by Silt monitoring and watershed modeling. In *Report Submitted to Ministry of Human Resources Department (MHRD)*; Department of Civil Engineering, IIT: Guwahati, India, 2005.

119. Wark, J.W.; Keller, F.J. Preliminary study of sediment sources and transport in the Potomac River basin. In *Technical Bulletin; Interstate Commission on the Potomac River Basin*: Rockville, MD, USA, 1963; 28p.
120. Yorke, T.H.; Herb, W.J. *Effects of Urbanization on Streamflow and Sediment Transport in the Rock Creek and Anacostia River Basins, Montgomery County, Maryland, 1962-74*; U.S. Geological Survey: Washington, DC, USA, 1978.

Disclaimer/Publisher's Note: The statements, opinions and data contained in all publications are solely those of the individual author(s) and contributor(s) and not of MDPI and/or the editor(s). MDPI and/or the editor(s) disclaim responsibility for any injury to people or property resulting from any ideas, methods, instructions or products referred to in the content.